Molecular Pharmacology Fast Forward. Published on February 9, 2005 as doi:10.1124/mol.104.008185

Title Page

Structural features of the glutamate binding site in recombinant NR1/NR2A *N*-methyl-D-aspartate receptors determined by site-directed mutagenesis and molecular modeling

Philip E. Chen, Matthew T. Geballe, Phillip J. Stansfeld, Alexander R. Johnston, Hongjie Yuan, Amanda L. Jacob, James P. Snyder, Stephen F. Traynelis and David J.A. Wyllie

Division of Neuroscience, University of Edinburgh, 1 George Square, Edinburgh EH8 9JZ, United Kingdom. PEC, PJS, ARJ, DJAW

Department of Chemistry, Emory University, 1515 Dickey Drive, Atlanta, Georgia 30322. MTG, JPS

Department of Pharmacology, Emory University School of Medicine, Rollins Research Center, 1510 Clifton Road, Atlanta, Georgia 30322. HY, ALJ, SFT

Running Title Page

Glutamate binding to NR1/NR2A NMDA receptors

Correspondence: David J A Wyllie

Division of Neuroscience

University of Edinburgh

1 George Square

Edinburgh

EH8 9JZ

United Kingdom

Tel: +44 131 650 4564

Fax: +44 131 650 6530

Email: dwyllie1@staffmail.ed.ac.uk

Number of text pages:	24
Number of Tables:	1
Number of Figures:	12
Number of References:	40
Words in Abstract:	249
Words in Introduction:	732
Words in Discussion:	1300

Abbreviations: NMDA, *N*-methyl-D-aspartate; AMPA, α -amino-3-hydroxy-5-methyl-4-isoxazole propionic acid; TEVC, two electrode voltage clamp; D-AP5, D-2-amino-5-phosphonopentanoic acid; MTSEA, methanethiosulfonate ethylammonium.

Abstract

We have used site-directed mutagenesis of amino acids located within the S1 and S2 ligand binding domains of the NR2A NMDA receptor subunit to explore the nature of ligand binding. Wild-type or mutated NR1/NR2A NMDA receptors were expressed in *Xenopus laevis* oocytes and studied using TEVC. We investigated the effects of mutations in the S1 and S2 regions on the potencies of the agonists L-glutamate, L-aspartate, RS-tetrazol-5-yl glycine and NMDA. Mutation of each of the corresponding residues found in the NR2A receptor subunit, suggested to be contact residues in the GluR2 AMPA receptor subunit, caused a rightward shift in the concentration-response curve for each agonist examined. None of the mutations examined altered the efficacy of glutamate as assessed by MTSEA potentiation of agonist-evoked currents. In addition none of the mutations altered the potency of glycine. Homology modeling and molecular dynamics were used to evaluate molecular details of ligand binding of both wild-type and mutant receptors, as well as to explore potential explanations for agonist selectivity between glutamate receptor subtypes. Our modeling studies support our interpretation of the mutagenesis data and indicate a similar binding strategy for L-glutamate and NMDA when they occupy the binding site in NMDA receptors as has been proposed for glutamate binding to the GluR2 AMPA receptor subunit. Furthermore, we offer an explanation as to why 'charge conserving' mutations of two residues in the binding pocket result in non-functional receptor-channels and suggest a contributing molecular determinant of why NMDA is not an agonist at AMPA receptors.

The NMDA receptor-channel is thought to be formed from the co-assembly of two NR1 subunits and two NR2 subunits in a dimer of dimers configuration (Schorge and Colquhoun, 2003). NMDA receptors are unique among ligand-gated ion channels in that the binding of two different ligands is required for the activation of the receptor-channel complex. Glycine, a co-agonist, binds to residues located in the NR1 subunits, whereas glutamate binds to residues located in NR2 subunits (reviewed by Erreger et al., 2004) of which there are four types (termed NR2A-D or epsilon 1-4) and which are the major determinants of the pharmacological and biophysical properties of these receptors (Monyer et al., 1992, 1994; Vicini et al., 1998; Wyllie et al., 1998). Ionotropic glutamate receptor subunits are comprised of distinct functional regions – an amino terminal domain, a ligand binding domain, a membrane-associated region and an intracellular carboxy terminal domain (see Fig. 1A). The ligand binding domain is thought to form a hinged clamshell-like structure (Armstrong et al., 1998) and is comprised of a region preceding the first membrane spanning domain (termed S1) and a region between the second and third membrane spanning domains (termed S2). In NR2 NMDA receptor subunits these regions show a high degree of homology with those located in AMPA and kainate receptor subunits and bacterial glutamate receptors (Paas, 1998; Chen et al., 1999). There is also similarity in sequence and predicted secondary structure between this region and ligand binding regions of bacterial periplasmic binding proteins (Oh et al., 1993, 1994).

X-ray diffraction studies have described the glycine binding domain of the NR1 subunit (Furukawa and Gouaux, 2003), but no equivalent structural data for any NR2 subunit exists, although some insights have been obtained from modeling studies (Chohan et al., 2000; Tikhonova et al., 2002; Laube et al., 2004). However, it is possible to make certain predictions about the nature of the contact residues in the NR2A NMDA receptor subunit with reference to studies of the AMPA receptor GluR2 S1S2 fragment (Armstrong et al.,1998;

Armstrong and Gouaux, 2000). Six residues in the GluR2 S1S2 construct are thought to hydrogen bond directly with glutamate, these being Pro478, Thr480 and Arg485 (S1 domain) and Ser654, Thr655 and Glu705 (S2 domain). In addition Tyr450 in GluR2 forms an electron-dense ring structure above the ligand binding site. Of the residues in GluR2, four are conserved in the homologous positions in NR2 (glutamate binding) NMDA receptor subunits with the exceptions being a histidine residue replacing Tyr450, a serine residue for Pro478 and an aspartic acid residue for Glu705 as indicated in sequence alignment shown in Fig. 1B. Figure 1C highlights the residues in the GluR2 and NR1 receptor subunits that participate in ligand binding and the corresponding residues in the NR2A NMDA receptor subunit (with their numbers). In the case of the GluR2 and NR2A subunit the numbering refers to the mature protein, while those numbers given for NR1 include the signal peptide (see Armstrong et al., 1998; Armstrong and Gouaux, 2000; Furukawa and Gouaux, 2003). A number of studies have reported that mutations of these residues in various NR2 subunits can alter glutamate potency (Williams et al., 1996; Laube et al., 1997; Anson et al., 1998; Chen et al., 2004; Kalbaugh et al., 2004; for a review see Erreger et al., 2004).

In this study we have systematically mutated all six of the predicted contact residues in either the S1 or S2 domains together with the histidine residue thought to play the same site-capping role as Tyr450 in GluR2 (Armstrong et al., 1998). We subsequently examined activation of mutant receptors that retained function by L-glutamate, L-aspartate, NMDA and RS-tetrazol-5yl-glycine, a potent NMDA receptor agonist (Schoepp et al., 1991). The structures of each of these agonists are shown in Fig.1D. Our results demonstrate that although each mutation causes a rightward shift in the concentration-response curve for each agonist, clear differences exist in the extent to which this occurs for each mutation and in the rank order of potency of agonists. To gain an insight as to how these different agonists interact with the ligand binding site in the NR2A subunit, we have constructed homology

models of the protein structure based on the crystal structure of the glycine-bound NR1 S1S2 protein fragment (Furukawa and Gouaux, 2003). We subsequently docked L-glutamate and NMDA into to putative ligand binding site based on the location of glycine in the NR1 structure.

Materials and Methods

Plasmid constructs, cRNA synthesis and receptor expression in oocytes. The wild-type pSP64T-derived expression plasmids for NR1 and NR2A NMDA receptor subunits were as described in Kuner and Schoepfer (1996). In this study we co-expressed various NR2 receptor subunits with the NR1-1a (exon 5 lacking, exon 21, 22 containing) subunit (Hollmann et al., 1993), which we will refer to as "NR1". Mutations were introduced into the NR2 subunit sequence using a PCR-based strategy. To assist with the subcloning and identification of the various constructs, some silent mutations were incorporated into the sequence encoding NR2A. PCR-generated DNA segments and subcloning sites were confirmed by DNA sequencing. cRNA was synthesized as runoff transcripts from linearized plasmid DNA using the Promega (Madison, WI) RiboMax RNA synthesis kit. Reactions were supplemented with 0.75 mM capping nucleotide m ^{7}G(5´)ppp(5´)G (Promega, Madison, WI) in the presence of 1.6 mM GTP. cRNA amounts and integrity were estimated by intensity of fluorescence in ethidium bromide-stained agarose gels, and concentration was determined also by OD_{260}. NR1 and NR2A cRNAs were mixed at a nominal ratio of 1:1 and diluted with water to 5 ng/µl of each, before injection.

Oocytes were obtained from *Xenopus laevis*, after administration of a lethal dose of anaesthetic (all procedures were carried out in accordance with current UK Home Office requirements). Prior to injection with cRNAs of interest, the follicular membranes of the oocytes were removed. After injection oocytes were placed in separate wells of 24-well plates

containing a modified Barth's solution with composition (in mM): NaCl 88, KCl 1, $NaHCO_3$ 2.4, $Ca(NO_3)_2$ 0.33, $MgCl_2$ 0.82, $CaCl_2$ 0.44, Tris-Cl 15, adjusted to pH 7.35 with NaOH (Sigma-Aldrich, UK). This solution was supplemented with 50 IU/ml penicillin and 50 mg/ml streptomycin (Invitrogen, UK). Oocytes were placed in an incubator (19 ^{o}C) for 24-48 hours to allow for receptor expression and then stored at 4˚C until they were used for electrophysiological measurements.

Electrophysiological Recordings and Solutions. TEVC recordings were made, using a GeneClamp 500 amplifier (Axon Instruments, Union City, CA), from oocytes that were placed in a modified frog Ringer solution that contained (in mM): NaCl 115, KCl 2.5, HEPES 10, $BaCl_2$ 1.8; pH 7.3 with NaOH (20 ºC) (Sigma-Aldrich, UK). Current and voltage electrodes were made from thin-walled borosilicate glass (GC150TF-7.5, Harvard Apparatus, Kent, UK) using a PP-830 electrode puller (Narashige Instruments, Japan) and when filled with 3 M KCl possessed resistances of between 0.5 and 1.5 MΩ. Oocytes were voltage-clamped at potentials of –40 mV. For L-glutamate, L-aspartate, NMDA and RS-tetrazol-5-yl glycine concentration-response measurements, the recording solution was further supplemented with 20 μM glycine and for glycine dose-response measurements this solution was supplemented with either 30 μM glutamate for wild-type receptors or 10 mM glutamate for mutant receptors. Glutamate receptor agonists were purchased from Tocris Cookson (Avonmouth, UK). Application of solutions was controlled manually and data were filtered at 10 Hz and digitized at 100 Hz. Test solutions were applied for 20 s or until a plateau to the agonist-evoked response had been achieved. The maximum agonist concentration applied to any oocyte was 30 mM as concentrations higher than this produced considerable changes in the osmolarity of the recording solution. The current response to a maximal agonist concentration for all constructs used here was always less than 3 μA at a holding potential of –40 mV. The open probability of NMDA receptors containing mutations in either the S1 or

S2 binding site was assessed by co-expressing these subunits with NR1 subunits carrying the A652C mutation (Jones et al., 2002; Yuan et al., 2005). Following the application of a maximal concentration of glutamate (+ 30 μM glycine) at a holding potential of –40 mV to oocytes expressing either wild-type or mutated NR2A receptor subunits the solution was switched to one containing glutamate, glycine and a maximally effective concentration of MTSEA (0.2 mM; Toronto Research Chemicals Inc., Toronto, Canada). The increase in the level of current recorded following the application of MTSEA was expressed relative to the current evoked in the absence of MTSEA.

Data analysis for dose-response curves. Data analysis of concentration response curves was performed using the program CVFit, available from: http://www.ucl.ac.uk/Pharmacology/dc.html. Dose-response curves were fitted individually for each oocyte with the Hill equation:

$$I = I_{max} / (1 + (EC_{50}/[A])^{n_H})$$

where n_H is the Hill coefficient, I_{max} is the maximum current, [A] is the concentration of agonist, and EC_{50} is the concentration of agonist that produces a half-maximum response. Each data point was then normalized to the fitted maximum of the dose-response curve. The normalized values were then pooled and averaged for each construct and fitted again with the Hill equation, with the maximum and minimum for each curve being constrained to asymptote to 1 and 0 respectively. A similar protocol was used to determine the concentration of the NMDA antagonist, D-AP5 required to inhibit a glutamate-evoked response by 50 % (IC_{50}). In these experiments the glutamate concentration was fixed at the concentration required to evoke a half-maximal response in the construct being investigated.

Modeling of the glutamate binding site in the NR2A NMDA receptor subunit. A homology model of the S1-S2 region of NR2A (GenBank Accession D13211) was constructed from the NR1-glycine crystal structure (1PB7; Furukawa and Gouaux, 2003)

using Modeller-3. The output of Modeller-3 was viewed in Sybyl (version 6.9) and compared to the template (NR1) to see if there were unacceptable backbone conformations. The model was further analyzed by Sybyl Protable to identify high-energy regions. These were eliminated by realigning the backbone through introducing gaps. The altered alignment increased the degrees of freedom of problematic regions and rotated side chains that were the basis for high energies. The new alignment was resubmitted to Modeller-3, and five iterations of viewing the model, changing the alignment and resubmitting to Modeller-3 were performed until the total energy of the modeled protein was minimized. The matchmaker energy of the final model (Sybyl) was –0.19kT, similar to that for the NR1 crystal structure (–0.23kT).

In order to generate a binding site without close contacts and with reasonable hydrogen bonds, the homology model was supplemented with MMFF94 force field charges and subjected to Sybyl (version 6.9) molecular dynamics (MD) for 5000 femtoseconds (fs) using an NTP ensemble (20 K and 1 atm). During the first stage of molecular dynamics only the backbone atoms of the protein were permitted to move. A second molecular dynamics run with identical parameters allowed only the side chain atoms to move. Finally, the agonist ligand and all amino acid residues within 6.0 Å of it were subjected to the same treatment. In this way, all poor contacts within the protein were removed, while the ligand adopted reasonable hydrogen-bonding interactions with the surrounding residues. This allowed the model to achieve a relatively strain-free conformation. Subsequently, separate protein-ligand models of L-glutamate and *N*-methyl-D-aspartate (NMDA) were created with ligand conformations that closely matched that of L-glutamate from the GluR2 site (protein data bank 1FTJ). These were loaded with MMFF94 charges and manually docked into the candidate agonist binding site using the match command and the GluR2 site as guidance. The individual ligand-protein systems were subjected to molecular dynamics simulation in Sybyl (version 6.9) using the TRIPOS force field (20 K, 1 atm, NTP ensemble, coupling constant 20), for

10,000 fs holding fixed all residues outside of a 6.0 angstrom radius around the ligand aggregate. To produce the final structures, the last 1000 fs of molecular dynamics was averaged and subsequently minimized with the Powell algorithm until an energy gradient of 0.01 kcal/mol was reached. The resulting structures were used to evaluate changes in binding site interactions caused by mutation of binding site residues.

For the mutation studies of R499K and D712E, modified structures were created using Sybyl's "modify/mutate" command on the optimized protein-ligand complexes described above. The mutated and liganded protein complexes were then subjected to the same molecular dynamics and energy minimization procedures employed for the native protein. All models can be downloaded from www.pharm.emory/straynelis/downloads.

Further analysis of both NMDA and L-glutamate in the GluR2 structure and the NR2A model was performed using the GROMACS molecular dynamics package (Lindahl et al., 2001). The protein and ligands were simulated using the Gromos96 force field and solvated with the spc water model. Each complex was energy minimized to remove any poor contacts, subjected to 20 ps of position restrained molecular dynamics to allow water to soak into the structure, and then 250 ps of unrestrained molecular dynamics at 300 K. An average structure was calculated from the last 100 ps of simulation and minimized to obtain a final structure.

Results

Steady-state agonist dose response curves were constructed by measuring the response to repeated application of increasing concentrations of each of the four agonists to oocytes held under voltage-clamp at –40 mV. The mean concentration response curves for each of the agonists, shown in Fig. 2, reveal a rank order of potency for these ligands at wild-type NR1/NR2A NMDA receptors as tetrazol-5yl-glycine > glutamate > aspartate > NMDA. The mean EC_{50} values for each agonist are given in Table 1. These values are in good agreement

with values obtained from various studies of native and recombinant NMDA receptors (for a review see Dingledine et al., 1999). In addition, the mean maximal currents evoked by each of the agonists were similar, these being 1.77 ± 0.34 μA (tetrazol-5yl-glycine), 1.42 ± 0.23 μA (glutamate), 1.64 ± 0.20 μA (aspartate) and 1.66 ± 0.17 μA (NMDA). Evaluation of responses to maximally effective concentrations suggests that agonist efficacy relative to glutamate for all compounds ranged between 89 – 97 % (data not shown).

The ligand binding site in the NR2A receptor subunit. We created a homology model of the NR2A S1-S2 ligand binding domain using the NR1-glycine crystal structure as a template (Furukawa and Gouaux, 2003). Figure 3A illustrates the alignment used to refine the homology model, while Fig. 3B shows the predicted bi-lobed structure of the NR2A subunit with glutamate docked in the ligand binding site. Figure 3C compares the known tertiary structures of NR1 and GluR2 with that of our model of the NR2A S1S2 binding domain. The primary difference between the NR2A construct and the NR1 and GluR2 crystallographic structures is the presence of several insertions, which are modeled as surface loops in NR2A. Glutamate and its analogues were docked into the NR2A model using the original description of glutamate binding to AMPA receptor S1-S2 (Armstrong and Gouaux, 2000) as a guide and molecular dynamics as a provisional refinement protocol (see *Materials and Methods*). Figure 4 summarizes the contact residues and proposed hydrogen bonding for glutamate and NMDA docked into the NR2A ligand binding pocket. As expected, all six residues proposed to participate in glutamate binding to AMPA receptors are involved in binding of docked L-glutamate within our model of NR2A (Fig. 4A,B upper panels). The alpha carboxyl is primarily anchored by Arg 499 plus backbone nitrogens from Thr494 and Ser670, identical to glutamate binding to GluR2. Arg499 also makes an important hydrogen bond with the backbone carbonyl of Thr494. The α-amino group appears secured by the backbone oxygen of Ser492, the sidechain of Thr494 and the carboxylate of Asp712, again in a fashion similar

to glutamate binding to GluR2. The γ-carboxyl interacts with the hydroxyl groups from Ser 670 and Thr671, with additional support from the Thr671 backbone nitrogen (Armstrong and Gouaux, 2000). As is the case with Tyr450 in the GluR2 subunit, His466, while not participating directly in hydrogen bonding with glutamate, appears to seal off the pocket from several well-packed hydrophobic residues behind it. The possible involvement of the histidine in a cation-π interaction is discussed below. Furthermore, residues homologous to all of those within NR1 in contact with glycine are involved in glutamate binding (Furukawa and Gouaux, 2003). These data further support the emerging idea that the glutamate recognition site in the NMDA NR2A receptor subunit binds glutamate by means of a pharmacophoric pattern very similar to that exhibited by other members of the glutamate receptor family.

We subsequently docked NMDA into our model of NR2A and found several notable differences in binding. Figure 4A,B (lower panels) illustrates predicted differences between NMDA and glutamate binding to NR2A. Overlays of glutamate and NMDA within the common NR2A binding pocket emphasize how two molecules with different stereochemistry still satisfy most of the same hydrogen bonded contacts. We predict that the decreased degrees of freedom for NMDA (and aspartate) compared to the more extended glutamate will reduce the importance of Ser670 and Thr671 for holding the ligand in the pocket. Not surprisingly, one of the main differences in binding contacts between glutamate and NMDA involves the addition of an N-methyl to NMDA. Our model suggests that replacement of hydrogen with methyl in this group not only alters the position of the ligand in the pocket, but may also promote a tighter interaction with the protein. While non-polar functionality carried by ligands is often seen as hydrophobic in nature, the methyl group of NMDA's N^{+}-Me offers something additional. Little recognized is the phenomenon that the charge in an N-methyl cation is not localized on nitrogen, but leaks out onto the hydrogens on carbon. Consequently,

each of these hydrogens bears a positive charge of approximately +0.2 to +0.3(Sun et al., 2005). Thus, in the NR2A receptor, the negatively charged carboxylates of the Glu394 (not shown in Figures 4 or 5) and Asp712 side chains surround the N-methyl group to provide productive electrostatic contacts. By contrast, in the GluR2 model the residues corresponding to the latter side chains are both Glu, but they are estimated to be situated approximately 1.5Å further away from the putative site. This suggests that they would make a diminished contribution to NMDA binding, if it was able to locate in the protein.

A molecular determinant of the selectivity of NMDA receptors. Despite the similarity in structure of the ligand binding pocket among the AMPA receptors GluR2, the glycine binding subunit NR1, and the glutamate binding subunit NR2A, important differences exist between these subunits in terms of their agonist selectivity. For example, NR1 cannot be activated by any glutamate analogues, whereas glutamate can activate both GluR2 and NR2A. Furukawa and Gouaux (2003) provided testable hypotheses regarding both steric constraints of the binding pockets as well as availability of hydrogen bonding contacts. D- and L-aspartate and its *N*-methyl D-isomer NMDA selectively bind to NR2A but do not activate GluR2 (data not shown), whereas glutamate can occupy both binding sites. In order to evaluate the basis for this selectivity, we superimposed the glutamate-bound GluR2 crystal structure (Fig. 5A) with our NMDA-bound NR2A (Fig. 5B). Two striking differences in the binding pockets suggest a basis for NR2A selectivity for NMDA. First, we predict that aspartate, one methylene group shorter than glutamate, cannot extend its carboxyl groups to interact with both Arg485 and Ser654/Thr655 in GluR2 (Armstrong and Gouaux, 2000). The distance between the α– and γ-carboxyl carbons in GluR2/glutamate (4.41 Angstroms) is greater than in NR2A/glutamate (3.70 Angstroms), while NR2A/NMDA shows a much shorter spacing between the same atoms (2.91 Angstroms). Thus, the geometry of the NR2A pocket can adapt to allow aspartate binding. Second, it is apparent from inspection of Fig.

5C,D that Met708 intrudes into the binding pocket of GluR2. This residue, which is conserved across the AMPA receptor family, and in the case of GluR2 adopts different conformations depending on the nature of the agonist occupying the binding site (Kasper et al., 2002), appears to reside in a position that may on occasion overlap, sterically, with the methyl group of NMDA, providing one explanation for non-optimal interaction of NMDA with AMPA receptors. Intriguingly, it has been suggested that this residue may play a role in determining agonist selectivity between AMPA and kainate receptors (Lunn et al., 2003). The analogous residue in NR2A (Val715) is smaller, and is predicted to extend along the main chain rather than protrude into the water filled pocket. Figure 5D illustrates this potential steric clash, and also shows differences between a model of NMDA binding to NR2A and experimentally determined glutamate binding to GluR2. In their recent study Laube et al. (2004) have also implicated the corresponding Val residue in NR2B (Val709) in ligand selectivity. Mutation of Val709 to a Met residue reduced NMDA potency by 22-fold. However, from our study of NR2A, the corresponding mutation, V715M, reduced NMDA potency by only around 2-fold, but increased glutamate potency by a similar amount (Fig. 5E,F). Therefore this mutation increases glutamate to NMDA selectivity by 4-fold. At first glance it is surprising that replacement of the corresponding residue in NR2A, Val715, with Met causes only a 2-fold decrease in NMDA potency. This can be understood by examining the disposition of the side chains on alpha-helix I, the locus of the residues at 708 and 715, respectively. In GluR2, the orientation of this helix causes Met708 to be unambiguously directed at the NMDA binding center, thereby preventing its docking in the protein. In NR2A, a slight tilt of the same helix causes two changes. The Met residue now introduced at position 715 is directed above the NMDA ligand. This is accompanied by the positioning of Tyr711 between Met715 and NMDA effectively blocking contact between the two entities. The Tyr711 orientation is assisted by H-bonding to Glu394. Given that in GluR2 Met708

participates in a hydrophobic network with several other S1 and S2 residues (Hogner et al., 2002) it remains to be established to what extent single residues can determine agonist selectivity. In the present case, however, it may be that a single mutation coupled to nearby alterations between NR2A and GluR2 cooperate to produce small but significant reorientations of secondary structure (i.e. alpha-helix I) that influences the function of an otherwise well-tuned binding pocket.

Mutation of contact residues in the S2 binding domain. To evaluate the contribution of contact residues to various ligand binding sites, we evaluated the effect of mutation at each contact residue on the concentration-response curve for all four ligands. We initially mutated two proposed uncharged contact residues Ser670 and Thr671 in the S2 domain of NR2A. The serine-threonine motif in the S2 binding domain of each of the NR2 NMDA receptor subunits is conserved in the GluR2 AMPA receptor subunit. It has been reported previously (Anson et al.,1998) that mutation of the serine located at position 670 in the NR2A receptor subunit to alanine residue (S670A) gives less than a 2-fold shift in glutamate potency, most likely due to the predicted backbone hydrogen bond with the γ-carboxyl that will be retained in the alanine mutant. This result is in contrast to the study of Laube et al. (1997) who reported that mutation of the homologous residue in the NR2B NMDA receptor subunit to glycine (S664G) reduces glutamate potency by 180-fold. Thus, we first made the equivalent serine to glycine mutation in the NR2A NMDA receptor subunit. Figure 6 shows representative two-electrode voltage-clamp current recordings for glutamate/glycine or NMDA/glycine activated currents mediated either by wild-type NR1/NR2A NMDA receptors (Fig 6A,C) or NR1/NR2A(S670G) NMDA receptors (Fig. 6B,D). Similar recordings were performed for aspartate and tetrazol-5yl-glycine evoked currents. The mean concentration response curves obtained for each of the agonists acting at NMDA receptors carrying either the NR2A(S670G) or NR2A(T671A) mutation are shown in

Fig. 7. To allow for ease of comparison and to indicate the degree of shift in potency we have superimposed the wild-type NR1/NR2A concentration response curves from Fig. 2. This data set shows that the biggest shifts in potency for NR1/NR2A(S670G) are seen with glutamate and aspartate (111-fold and 109-fold respectively; Fig. 7A,B), with smaller shifts observed for NMDA (12-fold, Fig. 7C) and tetrazol-5yl-glycine potency (21-fold, Fig. 7D).

Previous studies have characterized the properties of glutamate-activated NR1/NR2A(T671A) receptors and the homologous mutation in NR2D-containing NMDA receptors at both the whole-cell and single-channel level (Anson et al., 1998, 2000; Chen et al., 2004). In the present study, we find that the potencies for all four agonists were decreased by this mutation, with effects on glutamate potency being the largest (848-fold; Table 1). In the case of aspartate, a 100-fold shift in potency was observed (Fig.7B) whereas for NMDA and tetrazol-5yl-glycine the shifts in potency were 7-fold and 41-fold respectively (Fig. 7C,D). For each of these mutations in the S2 domain the rank order of potency of the agonists is altered from that observed for wild-type NR1/NR2A NMDA receptors. In the case of the NR2A(S670G) mutation the rank order of potency differs slightly from wild-type receptors, and is tetrazol-5yl-glycine > glutamate > NMDA > aspartate (i.e. NMDA and aspartate switch positions). By contrast, the NR2A(T671A) mutation the rank order of potency differs markedly from wild-type receptors, particularly with respect to glutamate: tetrazol-5yl-glycine > NMDA > aspartate > glutamate.

We interpret the effect on potency of the glycine, but not alanine, substitution at NR2A Ser670 as a likely indication of alterations in the geometry of the backbone chain. Glycine, which increases chain flexibility, may allow the chain to adopt conformations that hinder the ability of a hydrogen bond to form between the Ser670 chain nitrogen and the α-carboxyl. This interaction may help stabilize the other interactions of Ser670 and Thr671 with the γ-carboxyl (see Fig. 4). There is no obvious explanation for the 100-fold difference

between the potency of NMDA and glutamate for NR2A(T671A) containing receptors. Given a possible reduction in degrees of freedom and different orientations in the cleft, we predict that shorter D-aspartate based ligands may require less stabilization of their γ-carboxyl.

Mutation of residues in the S1 binding domain. Three uncharged residues in the S1 binding domain (H466, S492 and T494) were separately replaced with alanine by mutagenesis. Each of these residues is conserved in the four NR2 NMDA receptor subunits, while in the corresponding GluR2 AMPA subunit a tyrosine residue replaces histidine and a proline is found at the homologous position occupied by serine. Thr494 is conserved in each of these subunits as well as in the NR1 subunit (see Fig. 1B).

Figure 8 and Table 1 summarize the effects of mutating these S1 residues on agonist EC_{50} values. Each of the mutations investigated shifted the concentration response curves to the right for all agonists. The largest changes in potency were seen when aspartate was the agonist with both the S492A and T494A mutation each giving approximately 240-fold shifts. The biggest shift in potency for tetrazol-5yl-glycine was seen with the H466A mutation, T494A gave the biggest shifts in glutamate and aspartate potencies, while the biggest shift in NMDA potency was observed upon mutation of the Ser492 residue. In general these three mutations had less effect on tetrazol-5yl-glycine potency with only between 21- and 42-fold shifts in potency being observed when compared to wild-type receptors. We predict that tetrazol-5yl-glycine will show additional hydrogen bonds between the tetrazol ring and residues within the binding pocket (modeling data not shown), suggesting this agonist utilizes additional features of the binding pocket to stabilize its interactions. We interpret these additional interactions as stabilizing forces that counteract the loss of Ser492 and Thr494 interactions.

NR2A(S492A S670G) has additive effects on glutamate potency. We also investigated the effects of introducing two mutations in different lobes into the binding site of

the NR2A NMDA receptor subunit. The two double mutations chosen were NR2A(S492A S670G) and NR2A(T494A T671A). As is shown in Fig. 8E mutating both serine residues together causes a large shift in the potency of glutamate. The EC_{50} for NR2A(S492A S670G)-containing NMDA receptors is 4392 ± 695 μM (n = 6), corresponding to ~1500-fold reduction in glutamate potency. Mutation of the two threonine residues (Thr494 and Thr671) essentially abolished glutamate sensitivity, as only very small currents could be evoked by glutamate even when the concentration of agonist was raised to 30 mM. The ability of the double mutant to reduce potency further than each single mutant in isolation suggests that each of these mutations, individually, may not dramatically alter contacts of the other serine and threonine residues within the binding site.

Mutations in S1 and S2 domains do not affect agonist efficacy. Changes in the potency (EC_{50}) of an agonist at receptors carrying mutations are difficult to ascribe to changes in agonist binding if the mutation also affects the agonist's efficacy i.e. its ability to gate the channel (see Colquhoun, 1998). For this reason we present several lines of evidence as to why we consider the main effects of the mutations we have described above are to alter the ability of glutamate (and other agonists) to bind to the NMDA receptor.

First, to examine the ability of mutations in the S1 and S2 binding domains to affect the ability of glutamate to gate the channel once bound to the receptor we co-expressed wild-type and mutant NR2A subunits with NR1 subunits carrying the A652C mutation (Jones et al., 2002; Yuan et al., 2005). This mutation renders the NR1 subunit sensitive to the sulfhydryl-modifying reagent, MTSEA, which covalently modifies the receptor-channel causing it to adopt a locked open conformation. Thus the extent to which MTSEA potentiates currents evoked by a maximal agonist concentration gives a measure of the open probability of the channel. Figure 9(A-E) shows example currents recorded from oocytes expressing either wild-type NR2A subunits or subunits carrying mutations at the serine and threonine

residues located in the S1 (Fig. 9B,C) or S2 (Fig, 9D,E) regions. If MTSEA-modified channels are assumed to have an open probability near 1, the lack of difference in the degree of potentiation suggests that open probabilities are similar for unmodified mutant and wild-type receptors. Given that the mean potentiation (Fig. 9F) is around 2.3-fold for all receptors examined this suggests that the open probability for each of the constructs is about 0.4. This value is consistent with estimates of open probability for NR2A-NMDA receptors expressed in oocytes obtained from other studies using the MTSEA assay (Jones et al., 2003; Yuan et al., 2005) and from single-channel studies where the peak open probability of NR1/NR2A receptors has been measured directly and estimated to be 0.5 (Erreger et al., 2005; see also Wyllie et al., 1998). In control experiments (data not shown) MTSEA caused no potentiation in the absence of glutamate (+ glycine). In addition, when the various mutated NR2 subunits were co-expressed with wild-type NR1 receptor subunits MTSEA caused a slight degree of inhibition suggesting that MTSEA may act as channel blocker. The mean values for the percentage inhibition caused by MTSEA were: NR1/NR2A(S492A) 7.8 ± 2.7%; NR1/NR2A(T474A), 9.1 ± 3.0%; NR1/NR2A(S670G), 12.9 ± 4.6% and NR1/NR2A(T671A), 6.1 ± 2.1%; n = 9 – 12 oocytes per construct). These control data are consistent with previous reports on the effects of MTSEA (Jones et al., 2002; Yuan et al., 2005).

Second and in contrast to their effects on the potency for glutamate analogues, none of the mutations studied here affected the potency of glycine (Fig. 10A, Table 1). The similar EC_{50} values between glycine for wild-type and the receptors containing mutant NR2A receptor subunits (Table 1) suggests that changes in the binding energies within the pocket do not influence the allosteric interactions between the glutamate and glycine binding domains (Benveniste et al., 1990). The fact that the EC_{50} for glycine is not changed significantly in any of the mutant studies provides evidence that the shift in potency of glutamate is not mediated by a gross change in the gating characteristics of these channels. Previously it has

been shown that the equilibrium dissociation constant (K_B), determined by Schild analysis, for D-AP5 binding to NR1/NR2A(T671A) receptors is increased by around 250-fold (Anson et al., 1998) consistent with the notion that this mutation affects the binding site in the NR2A receptor subunit. While we have not undertaken experiments to determine the K_B for D-AP5 we have determined the concentration of this antagonist required to inhibit by 50 % the response evoked by a half maximal concentration of glutamate. The IC_{50} for D-AP5 acting at wild-type receptors was 0.37 ± 0.05 μM whereas this value increased significantly ($p < 0.05$) for each of mutants examined (NR2A(S492A), 4.4 ± 0.4 μM; NR2A(T464A), 2.3 ± 0.2 μM and NR2A(S670G), 1.2 ± 0.1 μM; n = 5 – 9 oocytes for each construct). Thus, this observed decrease in D-AP5 potency is consistent with the fact that these mutations affect the binding site of the NR2A subunit. The mean inhibition curves are shown in Fig.10B.

Finally, for each of the mutations made in either the S1 or S2 domain we did not observe > 5-fold changes in the maximal currents that were evoked in mutated NR2 subunits when compared to wild-type responses. The fact that large differences were not observed and also given that there were no significant decreases in the Hill Slopes (see Table 1) for each agonist studied is evidence in support of the notion that these mutations affect the ability of a ligand to bind to the NR2A subunit rather than alter its ability to gate the channel once it has bound. For glutamate-evoked currents the mean maximal currents were 1.4 μA (wild-type), 0.6 μA (H466A), 1.3 μA (S492A), 0.5 μA (T494A), 2.2 μA (S670G) and 2.0 μA (T671A).

Mutation of NR2A S1 residues to the homologous residues in NR1. Two of the proposed residues in the S1 domain, thought to participate in the binding of glutamate, vary between the NR2 and NR1 subunits; namely a serine at position 492 in NR2A (a proline residue in NR1 and GluR2) and a histidine at position 466 in NR2A (a phenylalanine residue in NR1). Our modeling studies suggest that the amino group of NMDA forms a hydrogen bond with the backbone oxygen of Ser492 (Fig. 4). Figure 11A-C shows the effect of the

mutation S492P on both NMDA and glutamate potency. When compared with the shifts in potency seen with the S492A mutation, the S492P mutation causes a greater shift in NMDA concentration response curves (potency shift is 75-fold compared with 30-fold, Fig. 11B), while the glutamate shift in potency is less (19-fold decrease in potency, compared with 42-fold decrease seen with S492A, Fig. 11C). The greater effect of NR2A(S492P) over NR2A(S492A) for NMDA compared to glutamate could reflect the loss or reduction of carboxylate stabilization by the α-amino in NMDA, implying an increased importance of the main chain oxygen for Ser492 stabilization of this group. The more likely perturbation of chain orientation with S492P (which will introduce a kink in the main chain) relative to S492A might explain the larger effect on NMDA potency.

His466 occupies a position analogous to Tyr450 in GluR2, and likely provides the binding pocket with a similar electron polarizable ring. Figure 11D-F shows the effect of mutating the histidine residue at position 466 to phenylalanine. In the case of both NMDA (Fig. 11E) and glutamate (Fig. 11F) the H466F mutation causes less of a potency shift than we observe with the H466A mutation (Table 1). This result is consistent with the idea that the ring structure of histidine plays an important role in stabilizing the ligand in the binding pocket. A particularly attractive explanation lies in the observation that these electron dense rings (His, Phe and Tyr) lie over the ammonium moieties of glutamate and NMDA depicted in Fig. 4A,B. It is well known that ammonium cations associate with electron rich aromatic rings in organic systems as well as proteins. These cation-π interactions (Dougherty, 1996; Ma and Dougherty, 1997) are sufficiently strong that they are energetically comparable with hydrogen bonds. Consequently, such an effect would be maintained by replacing His with Phe or Tyr. Since the strength of the interaction is related to both the distance of the cation from the ring center and the orientation of the π-cloud with respect to the cation, weaker

effects may arise as a result of ring twisting. The lower potency shift in the case of the H466F mutation may owe its origin to such a phenomenon.

NR2A(R499K) and NR2A(D712E) produce non-functional receptor-channels. Two of the six hypothetical contact residues in the binding site are charged. We introduced charge-conserving mutations at position 499 (arginine to lysine; R499K) and position 712 (aspartate to glutamate; D712E). When co-injected with cRNA for the NR1 NMDA receptor subunit neither of these constructs gave currents when glutamate was applied up to 10 mM. We also investigated whether any of the other three ligands used in this study might activate either NR2A(R499K)- or NR2A(D712E)- containing NMDA receptor-channels. In all cases each of these ligands failed to evoke a response in oocytes injected with these two constructs. It has previously been reported that both the equivalent arginine to lysine mutation in the NR2B NMDA receptor subunit (R493K; Laube et al., 1997) and the equivalent aspartate to glutamate mutation in NR2A/NR2B NMDA receptor subunits (D731E and D732E; Williams et al., 1996) give non-functional NMDA receptors. Figure 12A illustrates the critical role Arg499 plays in glutamate binding with the nearly planar orientation of guanidine and carboxylate groups engaged in double hydrogen bonding. Docking glutamate with the R499K mutant receptor further illustrates the importance of the interaction and the inability of Lys to substitute for Arg. Backbone interactions with the main chain limit the flexibility at this position such that Lys cannot extend to make the contacts that Arg can make.

In a separate vein, the NR2A model provides a satisfying interpretation of the consequences of replacing Asp712 with Glu. In the wild-type receptor Asp712 makes three coupled hydrogen bonds, two of which are to the neutral OH groups in the side chains of Ser492 and Tyr742 (not shown in Fig. 12B). The third interaction is with the cationic NH_3^+ of glutamate. The latter O(-)---(+)HN hydrogen bond is strongly reinforced by the oppositely charged centers. In the Glu712 mutant, the carboxylate still makes a pair of hydrogen bonds

to Ser492 and Tyr742. However, the electrostatically dominated H-bond is absent since the Glu residue's carboxylate unit is relocated away from the ligand. The loss of this important anchor to glutamate converts an ideal binding site a much less ideal one causing the ligand to be bound only weakly, if at all. A small polar side chain might restore an H-bond to the NH_3^+ of glutamate, but the weaker dipole-charge association is predicted to be insufficient to restore full receptor function (Fig. 12B). Several other studies have highlighted the importance of the Asp712 residue. Mutation of this sidechain in NR2A to either an Ala or Cys residue results in a non-functional channel (Williams et al., 1996; Kalbaugh et al., 2004) while the recent study of Laube et al. (2004) has indicated that mutation of the corresponding residue in the NR2B subunit to an Asn residue also abolishes receptor function. Thus it appears that conservative substitution (with Glu) or substitution with either small non-polar residues or polar residues each result in non-functional receptors. Hence these two non-functional mutations serve to illustrate important geometric constraints within the binding pocket.

Discussion

Effects of S1 and S2 mutations on agonist potency. Several structure-function studies of ionotropic glutamate receptors and related kainate binding proteins have identified residues located in the S1 and S2 binding domains that, when mutated, lead to a reduction in the ability of the ligand to remain bound to its binding site (for example see Kuryatov et al., 1994; Kuusinen et al., 1995; Paas et al., 1996; Laube et al., 1997, 2004; Anson et al, 1998, 2000; Wo et al., 1999; Kalbaugh et al., 2004; for a review see Erreger et al., 2004). This study is the first to describe, systematically, the effects of mutating each of the proposed contact residues in the ligand binding site of the NR2A NMDA receptor subunit and examine the effects of these mutations on several NMDA receptor agonists.

While shifts in the EC_{50} of a ligand for the activation of a receptor or a change in 'apparent affinity' of a ligand measured in a binding assay cannot indicate, definitively, that the mutation has had a direct effect on the microscopic rate constants determining binding (see Anson et al., 1998; Colquhoun, 1998) many of the residues identified in structure-function studies have been shown, from crystallographic studies (Armstrong et al., 1998; Armstrong and Gouaux, 2000; Furukawa and Gouaux, 2003) to hydrogen bond with glutamate receptor agonists. We have previously shown that mutation of Thr671 to alanine causes an increase in the equilibrium dissociation constant for the NMDA receptor antagonist, D-AP5, (Anson et al., 1998). Inasmuch as the agonist and antagonist binding sites overlap this can be taken as evidence that these mutations are altering binding of ligands. We have not carried out Schild analysis in this present study but have calculated IC_{50} values for D-AP5 which indicated that the potency of this antagonist is decreased when the serine and threonine residues in S1 and S2 are mutated to alanine residues (or glycine in the case of Ser670). Further evidence that the S1 and S2 mutations studied have their major effect on agonist binding rather than channel gating was obtained from our experiments with MTSEA. The extent of potentiation seen with MTSEA was similar for wild-type and each of the NR2A mutants indicating that the open probability of each of these NMDA receptors is similar. In these experiments the degree of potentiation is inversely correlated with the open probability of the receptor – receptors with a low open probability (such as NR2C- or NR2D-containing receptors) show greater potentiation following MTSEA application than do NMDA receptors with higher open probabilities (e.g. NR2A-containing receptors; see Yuan et al., 2005). Taken together these results support our hypothesis that the shifts in EC_{50} we report largely reflect changes in binding rates.

Each of the point mutations investigated in this study caused a decrease in potency for all agonists examined. However the degrees of shift observed were, in general, greater for

glutamate and aspartate than those for NMDA and tetrazol-5yl-glycine. Indeed the 'importance' of a residue in determining agonist potency varied greatly – for example the largest shift in glutamate potency (848-fold) occurs when Thr671 is mutated to an alanine residue but this mutation decreases NMDA potency by only 7-fold.

Even with knowledge that a residue is located in the binding pocket and is likely to hydrogen bond directly with glutamate, structure-function studies may miss, or place lesser emphasis on, a residue when only a small decrease in agonist potency is observed. This is exemplified when we consider the Ser670 residue in the S2 domain. In our present study we have shown that mutation of Ser670 to glycine, in the NR2A NMDA receptor subunit causes a far greater shift in potency than that seen when the residue is mutated to an alanine residue (Anson et al., 1998). This result might have been taken to suggest that Ser670 did not participate in agonist binding. Clearly this is not the case since when this residue was mutated to Gly a large shift was observed. In this respect the NR2A(S670G) mutation causes a similar shift in glutamate potency to that seen with the homologous mutation in the NR2B receptor subunit (Laube et al., 1997). As mentioned above the large shift in potency seen with the glycine but not alanine substitution at this position may result from the increased chain flexibility that occurs when glycine occupies this position. This may also be the case in the NR1 subunit with respect to glycine binding. At the equivalent position in the NR1 subunit, mutation of the serine residue (Ser688) to an alanine only produced a 4-fold reduction in glycine potency (Kuryatov et al., 1994). However the importance of this serine residue in glycine binding was only identified by the elucidation of the NR1S1S2 crystal structure (Furukawa and Gouaux, 2003). According to our observation of mutations in the NR2A subunit, we would predict that an equivalent serine to glycine mutation in the NR1 subunit would reduce, significantly, glycine potency.

Modeling of the binding site in the NR2A NMDA receptor subunit. A primary goal of this study is to provide functional data supporting the emerging idea that the glutamate binding site shares similar molecular features across the glutamate receptor family. The increasing availability of crystallographic data and homology modeling has increased the need for functional studies to substantiate and interpret data. Our experiments represent a systematic exploration of all proposed contact residues in a single NMDA subunit (NR2A). Furthermore, we studied four ligands at all mutant receptors, which provides additional insight into the nature of the binding pocket. Several clear themes emerge from these data. First, we find that the major molecular determinants of glutamate binding to GluR2 (see Armstrong and Gouaux, 2000) are present in the NR2A subunit. This reinforces the idea that the blueprint for ligand binding domains among glutamate receptors is largely shared not only through conserved amino acid residues comprising the domain but also within the contact residues that stabilize ligand binding. Second, there are specific molecular and geometric constraints on the NMDA receptor binding pocket. The ligand binding domain is not free to conform to any agonist with expected functional groups. Likewise, the tertiary structure cannot accommodate changes at critical residues that, for example, shorten side-chain length. This is most notable when we mutated the two charged residues in the binding site. Shortening the side chain length of Arg499 by changing this to lysine increases the distance between its side chain and the α-carboxyl of glutamate to such an extent that it cannot hydrogen bond. Similarly increasing the amount to which the γ-carboxyl of the residue at position 712 protrudes into the binding site by swapping the aspartate residue for glutamate indicates that length of the side chain at this position is critical for a functional receptor. Third, we describe several hypothetical features of the NMDA receptor binding pocket that define its selectivity for aspartate derivatives compared to AMPA receptors. Finally we propose that the differential contribution of residues to stabilization of different ligands

explains the differing effects of mutants on the rank order of potency – for example the relatively small shifts in potency of tetrazol-5yl-glycine may result from its ability to hydrogen bond with (additional) groups in the binding site which counteract the loss of the sites utilized by the other ligands.

Summary. Although these conclusions appear straightforward and predictive, we are aware of the limitations of homology modeling, particularly for the glutamate binding pocket which shows a number of interesting features we have neglected. Specifically, we have not included potential water bridged interactions in the pocket, and at times needed to choose between one of several possible orientations for side chains. Despite these caveats, the data presented here answer several longstanding questions about glutamate receptor pharmacology, and make a number of predictions that will help focus additional questions and experiments on the glutamate receptor-binding domain.

Acknowledgements

We thank Dr Lonnie Wollmuth for sharing the NR1(A652C) mutant with us, Dr Harry Olverman for suggesting the use of tetazol-5yl-glycine to probe receptor function and Dr Kris Dickson for valuable comments on the manuscript. MTG and JPS owe Prof Dennis Liotta gratitude for support and encouragement. In addition, we thank our colleagues at Edinburgh and Emory Universities with whom we have had helpful discussions during the course of this project.

References

Anson LC, Chen PE, Wyllie DJA, Colquhoun D and Schoepfer R (1998) Identification of amino acid residues of the NR2A subunit that control glutamate potency in recombinant NR1/NR2A NMDA receptors. *J Neurosci* **18:**581-589.

Anson LC, Schoepfer R, Colquhoun D and Wyllie DJA (2000) Single-channel analysis of a NMDA receptor possessing a mutation in the region of the glutamate binding site. *J Physiol* **527:**225-237.

Armstrong N, Sun Y, Chen GQ and Gouaux E (1998) Structure of a glutamate-receptor ligand-binding core in complex with kainate. *Nature* **395:**913-917.

Armstrong N and Gouaux E (2000). Mechanisms for activation and antagonism of an AMPA-sensitive glutamate receptor: crystal structures of the GluR2 ligand binding core. *Neuron* **28:** 165-181.

Benveniste M, Clements J, Vyklicky L Jr and Mayer ML (1990) A kinetic analysis of the modulation of N-methyl-D-aspartic acid receptors by glycine in mouse cultured hippocampal neurones. *J Physiol* **428**:333-57.

Chen GQ, Cui C, Mayer ML and Gouaux E (1999) Functional characterization of a potassium-selective prokaryotic glutamate receptor. *Nature* **402**:817-21.

Chen PE, Johnston AR, Mok MHS, Schoepfer R and Wyllie DJA (2004) Influence of a threonine residue in the S2 ligand binding domain in determining agonist potency and deactivation rate of recombinant NR1a/NR2D NMDA receptors. *J Physiol* **558:**45-58.

Chohan KK, Wo ZG, Oswald RE and Sutcliffe MJ (2000) Structural insights into NMDA ionotropic glutamate receptors via molecular modeling. *J Mol Model* **6**: 16-25.

Colquhoun D (1998). Binding, gating, affinity and efficacy: The interpretation of structure-activity relationships for agonists and of the effects of mutating receptors. *Brit J Pharm* **125:** 924-947

Dingledine R, Borges K, Bowie D and Traynelis SF (1999) The glutamate receptor ion channels. *Pharmacol Rev* **51:**7-61.

Dougherty, DA (1996) Cation-π Interactions in Chemistry and Biology: A New View of Benzene, Phe, Tyr, and Trp. *Science* **271**:163-168.

Erreger K, Chen PE, Wyllie DJA and Traynelis SF (2004) Glutamate receptor gating. *Critical Reviews in Neurobiology* **16**:187-224.

Erreger K, Dravid SM, Banke TG, Wyllie DJA and Traynelis, SF (2005) Subunit specific gating controls rat recombinant NR1/NR2A and NR1/NR2B channel kinetics and synaptic signalling profiles. *Journal of Physiology* in the press.

Furukawa H and Gouaux E (2003) Mechanisms of activation, inhibition and specificity: crystal structures of the NMDA receptor NR1 ligand-binding core. *EMBO J* **22:**2873-2885.

Hogner A, Kastrup JS, Jin R, Liljefors T, Mayer ML, Egebjerg J, Larsen IK and Gouaux E (2002) Structural basis for AMPA receptor activation and ligand selectivity: crystal structures of five agonist complexes with the GluR2 ligand-binding core. *J Mol Biol* 322:93-109.

Hollmann M, Boulter J, Maron C, Beasley L, Sullivan J, Pecht G, Heinemann S (1993) Zinc potentiates agonist-induced currents at certain splice variants of the NMDA receptor. *Neuron* **10**:943-954.

Jones KS, VanDongen HM and VanDongen AM (2002) The NMDA receptor M3 segment is a conserved transduction element coupling ligand binding to channel opening. *J Neurosci* **22**:2044-2053

Kalbaugh TL, VanDongen HMA and VanDongen AMJ (2004) Ligand-binding residues integrate affinity and efficacy in the NMDA receptor. *Mol Pharm* **66:**209-219.

Kasper C, Lunn ML, Liljefors T, Gouaux E, Egebjerg J and Kastrup JS (2002) GluR2 ligand-binding core complexes: importance of the isoxazolol moiety and 5-substituent for the binding mode of AMPA-type agonists. *FEBS Lett* 531:173-178.

Kuner T and Schoepfer R (1996) Multiple structural elements determine subunit specificity of Mg^{2+} block in NMDA receptor channels. *J Neurosci* **16:**3549-58.

Kuryatov A, Laube B, Betz H and Kuhse J (1994) Mutational analysis of the glycine-binding site of the NMDA receptor: structural similarity with bacterial amino acid-binding proteins. *Neuron* **12**:1291-1300.

Kuusinen A, Arvola M and Keinanen K (1995) Molecular dissection of the agonist binding site of an AMPA receptor. *EMBO J* **14:** 6327-6332.

Laube B, Hirai H, Sturgess M, Betz H and Kuhse J (1997) Molecular determinants of agonist discrimination by NMDA receptor subunits: analysis of the glutamate binding site on the NR2B subunit. *Neuron* **18:**493-503.

Laube B, Schemm R and Betz B (2004) Molecular determinants of ligand discrimination in the glutamate-binding pocket of the NMDA receptor. *Neuropharmacology* **47**:994-1007.

Lindahl, E, Hess B and van der Spoel D (2001) GROMACS 3.0: A package for molecular simulation and trajectory analysis. *J. Molec Mod* **7**:306-317.

Lunn ML, Hogner A, Stensbol TB, Gouaux E, Egebjerg J and Kastrup JS (2003) Three-dimensional structure of the ligand-binding core of GluR2 in complex with the agonist (S)-ATPA: implications for receptor subunit selectivity. *J Med Chem* 46:872-875.

Ma JC and Dougherty DA (1997) The Cation-π Interaction. *Chem Rev* **5**:1303-1324.

Monyer H, Sprengel R, Schoepfer R, Herb A, Higuchi M, Lomeli H, Burnashev N, Sakmann B and Seeburg PH (1992) Heteromeric NMDA receptors: Molecular and functional distinctions of subtypes. *Science* **256:**1217 - 1221.

Monyer H, Burnashev N, Laurie DJ, Sakmann B and Seeburg PH (1994) Developmental and regional expression in the rat brain and functional properties of four NMDA receptors. Neuron **12**:529-40.

Oh BH, Pandit J, Kang CH, Nikaido K, Gokcen S, Ames GF and Kim SH (1993) Three-dimensional structures of the periplasmic lysine/arginine/ornithine-binding protein with and without a ligand. *J Biol Chem* **268**:11348 –11355.

Oh BH, Kang CH, De Bondt H, Kim SH, Nikaido K, Joshi AK and Ames GF (1994) The bacterial periplasmic histidine-binding protein. Structure/function analysis of the ligand-binding site and comparison with related proteins. *J Biol Chem* **269**:4135– 4143.

Paas Y, Eisenstein M, Medevielle F, Teichberg VI and Devillers-Thiery A (1996) Identification of the amino acid subsets accounting for the ligand binding specificity of a glutamate receptor. *Neuron* **17**: 979-990.

Paas Y (1998) The macro- and microarchitectures of the ligand-binding domain of glutamate receptors. *Trends Neurosci* 21:117-25.

Schoepp DD, Smith CL, Lodge D, Millar JD, Leander JD, Sacaan AI and Lunn WH (1991) D,L-(tetrazol-5-yl)glycine a novel and highly potent NMDA receptor agonist. *Eur J Pharmacol* **203:**237-243

Schorge S and Colquhoun D (2003) Studies of NMDA receptor function and stoichiometry with truncated and tandem subunits. *J Neurosci* **23**:1151-1158.

Sun A, Lankin DC, Hardcastle K and Snyder JP (2005) 3-Fluoropiperidines and *N*-Methyl-3-fluoropiperidinium Salts: The Persistence of Axial Fluorine. *Chemistry Eur. J.* in the press.

Tikhonova IG, Baskin II, Palyulin VA, Zefirov NS and Bachurin SO (2002) Structural basis for understanding structure-activity relationships for the glutamate binding site of the NMDA receptor. *J Biol Chem* **18**:3836-3843.

Vicini S, Wang JF, Li JH, Zhu WJ, Wang YH, Luo JH, Wolfe BB and Grayson DR (1998). Functional and pharmacological differences between recombinant N-methyl-D-aspartate receptors. *J Neurophysiol* **79:** 555-566.

Williams K, Chao J, Kashiwagi K, Masuko T and Igarashi K (1996) Activation of N-methyl-D-aspartate receptors by glycine: Role of an aspartate residue in the M3-M4 loop of the NR1 subunit. *Mol Pharm* **50:**701-708.

Wo ZG, Chohan KK, Chen H, Sutcliffe MJ and Oswald RE (1999) Cysteine mutagenesis and homology modeling of the ligand-binding site of a kainate-binding protein. *J Biol Chem* **274**: 37210-37218.

Wyllie DJA, Béhé P and Colquhoun D (1998) Single-channel activations and concentration jumps: comparison of recombinant NR1a/NR2A and NR1a/NR2D NMDA receptors. *J Physiol* **510:** 1-18.

Yuan H, Erreger K, Dravid SM and Traynelis, SF (2005) Conserved structural and functional control of NMDA receptor gating by transmembrane domain M3. *J Biol Chem* (submitted)

Footnotes

This work was supported by the National Institutes of Health and NARSAD (SFT), the Biotechnology and Biological Sciences Research Council (DJAW) and The Wellcome Trust (DJAW).

Legends for Figures

Figure 1. A, cartoon sketch of an ionotropic glutamate receptor subunit showing the proposed membrane topology of three membrane spanning domains (M1, M3 and M4) and a re-entrant loop (M2) and the location of the amino terminal domain (ATD) and carboxy terminal domain (CTD). The ligand binding domain is formed by the S1 and S2 regions of the protein which come together to form a hinged clamshell-like structure. B, Sequence alignment of GluR2, NR2A-D and NR1 receptor subunits. In the case of GluR2 and NR1 the amino acids shown in bold type are those thought to hydrogen bond directly with glutamate (in the case of GluR2) or glycine (in the case of NR1). The amino acids located in the homologous positions of NR2 NMDA receptor subunits are also shown. In the case of GluR2 and NR2A-D sequences, the numbering refers to the position of the amino acid in the mature protein (i.e. the signal peptide has been removed) whereas the numbering for the NR1 sequence includes the signal peptide. Thus the numbering of the GluR2 and NR1 subunits is consistent with that used by Armstrong and Gouaux (2000) and by Furukawa and Gouaux (2003) respectively. The * symbol denotes the location of a residue whose side-chain contains an electron-dense ring structure which in the case of the GluR2 and NR1 subunit is thought to form a 'lid' to the binding pocket. The # symbol denotes the location of the methionine residue in the GluR2 subunit which our modeling studies predict causes a steric hindrance to the binding of NMDA to this subunit (see Fig. 5). C, residues and their corresponding positions in the GluR2, NR1 and NR2A receptor subunits thought to either participate in the binding of ligand or determine ligand selectivity. D, structure of the ligands used in the present study.

Figure 2. Mean concentration response curves for tetrazol-5yl-glycine (●), glutamate (■), aspartate (▲) and NMDA (◆). Data were fitted with the Hill Equation as described in

Materials and Methods. Data points are the means and standard deviations of between six and twenty four measurements.

Figure 3. A, sequence alignment used to generate the homology model (see *Materials and Methods*). In the amino acid sequence shown for NR1 the red-colored residues represent the β strands and the blue-colored residues are α helices (as described by Furukawa and Gouaux, 2003). B, overview of the bi-lobed clamshell structure and glutamate binding residues in NR2A model. In this panel, and also in panels C and D, the S1 domain is shown in orange, while the S2 domain is depicted in green. C, comparison of the main chain structure for NR2A model with the known structure of NR1 (1PB7). D, comparison of the main chain structure for NR2A model with the known structure of GluR2 (1FTJ).

Figure 4. A,B, different views of glutamate or NMDA docked into a homology model of the NR2A ligand binding domain. C, overlay of NMDA and glutamate in NR2A ligand binding domain. The S1 and S2 domains are shown in orange and green respectively (as in Fig. 3).

Figure 5. A, surface profile of the binding pocket of GluR2 with glutamate docked. B, surface profile of the binding pockets of NR2A with NMDA docked. C, superimposition of GluR2 (with glutamate docked) and NR2A (with NMDA docked) to illustrate the that Met708 may hinder, sterically, the binding of NMDA to the GluR2 binding pocket. D, ball and stick representation of the panel shown in C. In this illustration the GluR2 backbone is shown in gray with the amino acids pertaining to the GluR2 subunit numbered in white (on black background). The S1 and S2 domains of the NR2A subunit are shown in orange and green respectively and the homologous amino acids to those found in GluR2 labeled in green. E, F, concentration response curves for glutamate and NMDA evoked currents in oocytes

expressing either wild-type NR1/NR2A (■) or NR1/NR2A(V715M) (●) NMDA receptors. In the case of glutamate the NR2A(V715M) mutation results in an increase in glutamate potency (EC_{50} = 1.7 ± 0.1 μM, n_H = 1.3 ± 0.1, n = 5) and a decrease in NMDA potency (EC_{50} = 78 ± 6 μM, n_H = 1.3 ± 0.1, n = 5).

Figure 6. Representative two electrode voltage-clamp recordings obtained from oocytes held at a potential of –40 mV. A, C, currents evoked by glutamate or NMDA (in the presence of 20 μM glycine) at the concentrations indicated above each trace in oocytes expressing wild-type NR1/NR2A NMDA receptors. B, D, glutamate or NMDA evoked currents obtained from oocytes expressing NMDA receptors carrying a point mutation in the S2 domain where the serine residue at position 670 has been replaced with a glycine residue. Note that the relative shift in potency observed for glutamate-evoked currents is greater than that seen with NMDA-evoked responses.

Figure 7. Effects of mutating residues in the S2 region on agonist potency. A, mean concentration response curves for glutamate evoked currents in oocytes expressing either wild-type NR1/NR2A (■), NR1/NR2A(S670G) (●) or NR1/NR2A(T671A) (▲) NMDA receptors. B, C, D, average concentration response curves for aspartate, NMDA and tetrazol-5-yl-glycine respectively.

Figure 8. Effects of mutating residues in the S1 region on agonist potency. A, mean concentration response curves for glutamate evoked currents in oocytes expressing either wild-type NR1/NR2A (■), NR1/NR2A(H466A) (▼), NR1/NR2A(S492A) (◆) or NR1/NR2A(T494A) (⬢) NMDA receptors. B, C, D, average concentration response curves for aspartate, NMDA and tetrazol-5-yl-glycine respectively. E, effects of double mutations on

glutamate potency. NMDA receptors containing NR2A(S492A S670G) subunits causes a 1500-fold shift to the right in glutamate potency, whereas the mutation NR2A(T494A T671A) essentially abolishes glutamate sensitivity.

Figure 9. MTSEA potentiation of currents mediated by wild type or mutant NR2A subunits co-expression with NR1(A652C). A-E, examples of TEVC currents recorded from oocytes expressing either wild-type or mutant NMDA receptors. Glutamate, at a maximal concentration for each construct, was co-applied with 30 μM glycine before the addition of a solution containing MTSEA (0.2 mM), as indicated by the thicker bar above each trace. For comparison the currents have been illustrated with the glutamate-evoked currents for each construct scaled to similar sizes. Upper dashed lines indicate the baseline currents and the lower dashed lines the level of the glutamate-evoked current from which the MTSEA potentiation was measured. F, bar graph showing the mean potentiation for each construct with the number of oocytes contributing indicated above each bar. The degree of potentiation is expressed as the magnitude of the current recorded in the presence of MTSEA (I_{MTSEA}) divided by the magnitude of the current evoked by glutamate (+glycine) alone ($I_{Glu/Gly}$). There is no significant difference in the degree of potentiation seen with the various constructs (p = 0.3, one way ANOVA) with the values being: NR2A(WT) = 2.3 ± 0.1 fold, 50 μM glutamate; NR2A(S492A) = 2.6 ± 0.2 fold, 1.5 mM glutamate; NR2A(T494A) = 2.3 ± 0.1 fold, 5 mM glutamate; NR2A(S670G) = 2.4 ± 0.1 fold, 5 mM glutamate and NR2A(T671A) = 2.3 ± 0.1 fold, 30 mM glutamate.

Figure 10. Effects of S1 and S2 mutations on glycine and D-AP5 potency. A, mean concentration response curves for glycine recorded in the presence of a maximal concentration of glutamate from oocytes expressing either wild-type NR1/NR2A (■),

NR1/NR2A(H466A) (▼), NR1/NR2A(S492A) (◆), NR1/NR2A(T494A) (⬢), NR1/NR2A(S670G) (●) or NR1/NR2A(T671A) (▲) NMDA receptors. B, mean inhibition concentration-response curves for the antagonist, D-AP5, to assess its potency in blocking glutamate-induced currents.

Figure 11. NR2A(S492P) and NR2A(H466F) concentration response curves. A, representative two-electrode voltage-clamp recording obtained from an oocyte expressing NR1/NR2A(S492P) NMDA receptors in which the current was evoked by NMDA at the concentrations indicated. B, mean concentration response curve for NMDA-evoked currents in oocytes expressing NR1/NR2A(S492P) NMDA receptors. Note that the shift in NMDA potency seen with this mutation is greater than that observed with the S492A mutation (dashed line). C, mean concentration response curve for glutamate-evoked currents in oocytes expressing NR1/NR2A(S492P) NMDA receptors. In this case the shift in glutamate potency is less than that observed in oocytes expressing NR1/NR2A(S492A) NMDA receptors (dashed line). D, representative two-electrode voltage-clamp recording obtained from an oocyte expressing NR1/NR2A(H466F) NMDA receptors in which the current was evoked by NMDA at the concentrations indicated. E, F, mean concentration response curve for NMDA-evoked (E) or glutamate-evoked (F) currents in oocytes expressing NMDA NR2A receptor subunits carrying the H466F mutation. For both agonists the shift in their potencies is less than that observed with the NR2A(H466A) mutation (shown as dashed line).

Figure 12. A, comparison of glutamate docked into the wild type NR2A subunit (upper panel) or the NR2A(R499K) mutant subunit (lower panel). In the lower panel is can be seen that the effect of this mutation is to increase the distance between the α-carboxyl group of glutamate and the side chain of lysine to an extent that hydrogen bonding may not occur. B,

comparison of glutamate docked into the wild type NR2A subunit (upper panel) or the NR2A(D712E) mutant subunit (lower panel). In this case the increase in the chain length results in the loss of hydrogen bonding between amino and carboxyl groups.

Tables

Table 1. Mean EC_{50} values, Hill Slopes and shifts in potency for wild-type NR1/NR2A NMDA receptors and receptors carrying mutations in the S1 and S2 ligand binding domains. The number of oocytes studied is given in parenthesis.

Agonist	Glutamate	Aspartate	NMDA	Tet-gly	Glycine
Construct	EC_{50} (μM) n_H	EC_{50} (μM) n_H	EC_{50} (μM) n_H	EC_{50} (μM) n_H	EC_{50} (μM) n_H
Wild-type	3.5 ± 0.4	18.4 ± 1.4	47.0 ± 2.7	1.7 ± 0.2	2.6 ± 0.2
	1.2 ± 0.1 (*24*)	1.0 ± 0.1 (*10*)	1.5 ± 0.1 (*5*)	1.3 ± 0.2 (*6*)	1.5 ± 0.2 (*4*)
H466A	490 ± 64	1798 ± 391	3995 ± 93	71.1 ± 9.3	3.7 ± 0.2
	1.5 ± 0.2 (*7*)	1.3 ± 0.2 (*9*)	2.4 ± 0.2 (*6*)	1.3 ± 0.2 (*10*)	1.5 ± 0.1 (*4*)*
H466F	46.2 ± 3.2	--	229 ± 21	--	--
	1.7 ± 0.2 (*4*)		1.4 ± 0.2 (*7*)		
S492A	146 ± 7	4408 ± 277	1389 ± 157	35.7 ± 5.4	2.5 ± 0.3
	1.2 ± 0.1 (*6*)	0.9 ± 0.1 (*12*)	1.4 ± 0.2 (*5*)	1.1 ± 0.1 (*6*)	1.3 ± 0.2 (*5*)
S492P	68.0 ± 6.4	--	3545 ± 211	--	--
	1.4 ± 0.2 (*10*)		1.6 ± 0.1 (*9*)		
T494A	482 ± 38	4488 ± 382	552 ± 78	38.5 ± 4.5	1.5 ± 0.2
	1.3 ± 0.1 (7)	0.9 ± 0.1 (*12*)	1.2 ± 0.2 (*5*)	1.4 ± 0.2 (*6*)	1.2 ± 0.2 (*4*)
S670G	421 ± 58	1999 ± 114	544 ± 19	36.1 ± 3.2	2.3 ± 0.1
	1.4 ± 0.2 (*12*)	1.0 ± 0.1 (*12*)	2.1 ± 0.2 (*6*)	1.6 ± 0.2 (*8*)	1.3 ± 0.1 (*5*)
T671A	2967 ± 279	1851 ± 129	351 ± 25	69.6 ± 6.1	2.9 ± 0.2
	1.3 ± 0.1 (*5*)*	1.1 ± 0.1 (*16*)	2.2 ± 0.4 (*6*)	1.2 ± 0.1 (*6*)	1.3 ± 0.1 (*4*)*
			Fold-shift in EC_{50}		
H466A	140	98	85	42	
H466F	13		5		
S492A	42	240	30	21	
S492P	19		75		
T494A	138	244	12	23	
S670G	120	109	12	21	
T671A	848	101	7	41	

* values reported in Anson et al. (1998).

A

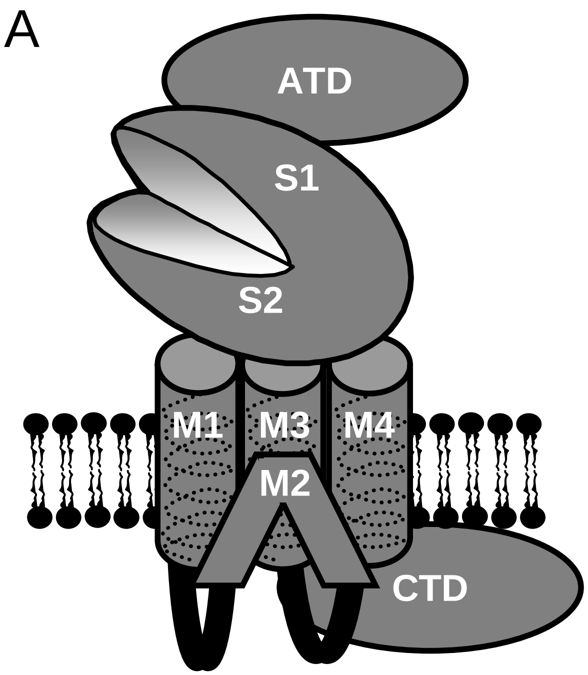

B

S1 domain

		*		
GluR2	446	GDGKYGARDADT	475	AIAPLTITLVREEV
NR1	480	ADGKFGTQERVN	513	IVAPLTINNERAQY
NR2A	462	TNGKHGKKVNNV	489	AVGSLTINEERSEV
NR2B	456	TNGKHGKKINGT	483	AVGSLTINEERSEV
NR2C	460	TNGKHGKRVRGT	487	AVGSLTINEERSEI
NR2D	480	TNGKHGKKIDGV	507	AVGSLTINEERSEI

S2 domain

				#
GluR2	648	GTLDSGSTKEFF	700	YAYLLESTMNEYIE
NR1	682	ATVKQSSVDIYF	727	HAFIWDSAVLEFEA
NR2A	664	GTVPNGSTERNI	707	DAFIYDAAVLNYKA
NR2B	658	GTVPNGSTERNI	701	DAFIYDAAVLNYMA
NR2C	662	GTVPNGSTERNI	705	DAFIYDAAVLNYMA
NR2D	685	GTVPNGSTEKNI	728	DAFIYDAAVLNYMA

C

Comparison of numbering of
'homologous' residues in iGluR subunits

GluR2		NR1		NR2A	
Tyr450	=	Phe484	=	His466	S1
Pro478	=	Pro516	=	Ser492	S1
Thr480	=	Thr518	=	Thr494	S1
Arg485	=	Arg523	=	Arg499	S1
Ser654	=	Ser688	=	Ser670	S2
Thr655	=	Val689	=	Thr671	S2
Glu705	=	Asp732	=	Asp712	S2
Met708	=	Val735	=	Val715	S2

D

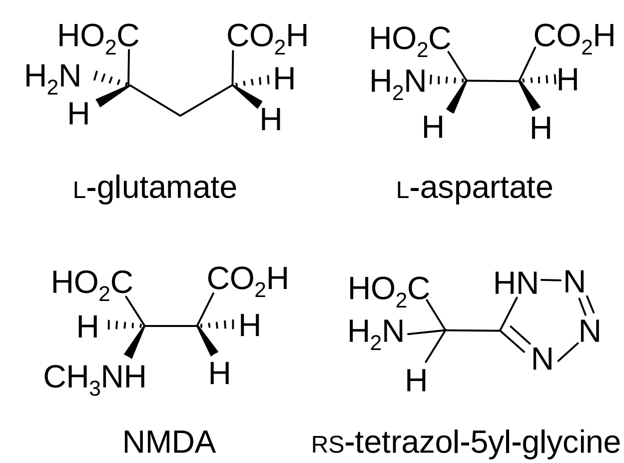

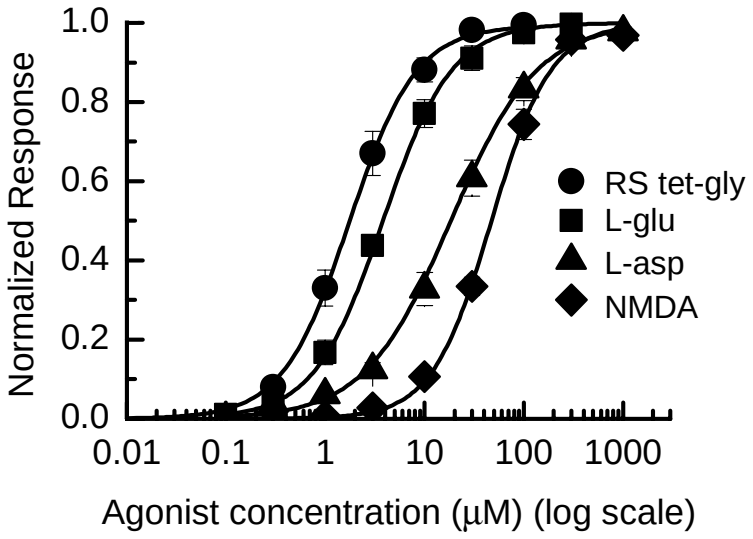
1.0
0.8
0.6
0.4
0.2
0.0
Normalized Response
0.01
0.1
1
10
100
1000
Agonist concentration (μM) (log scale)
RS tet-gly
L-glu
L-asp
NMDA

A

```
NR1  396 TRLKIVTIHQEPFVYVKPTMSD---GTCKEEFTVNGDPVKKVICTGPNDTSPGSPRHTVPQCCYGFCIDLLIKLARTMNFTY
NR2A 386 -HLSIVTLEEAPFVIVEDID--PLTETC-----VRNTVPCR-KFVKINNSTNEG-MNV-KKCCKGFCIDILKKLSRTVKFTY

NR1  475 EVHLVADGKFGTQERVNNSNKKEWNGMMGELLSGQADMIVAPLTINNERAQYIEFSKPFKYQGLTILVKK/RITGINDPRLR
NR2A 457 DLYLVTNGKHGKKVNN------VWNGMIGEVVYQRAVMAVGSLTINEERSEVVDFSVPFVETGISVMVSR/QVTGLSDKKFQ

NR1  674 NP---SDKFIYATVKQSSVDIYFR-RQVELSTMYRHMEKHNYESAAEAIQAVRDNKLHAFIWDSAVLEFEASQK--CDLVTT
NR2A 653 RPHDYSPPFRFGTVPNGSTERNIRN---NYPYMHQYMTRFNQRGVEDALVSLKTGKLDAFIYDAAVLNYKAGRDEGCKLVTI

NR1  750 G--ELFFRSGFGIGMRKDSPWKQNVSLSILKSHENGFMEDLDKTWVRYQECDS*
NR2A 732 GSGYIFATTGYGIALQKGSPWKRQIDLALLQFVGDGEMEELETLWLTG-ICHN*
```

Segments marked above NR1: 1 (KIVT), 2 (YVKP), 3 (VICT), 4 (PQCCY), B (FCIDLLIKLARTM), 5 (EVHL), 6 (QER), 7 (KEW), C (GMMGELL), 8 (MI), D (NERA), 9 (IEF), 10 (KYQGLTILVK), E (PRLR), 11 (YA), F (SVDIYFR), G (VELSTMYRHM), H (AAEAIQAVR), 12 (AFIWD), I (SAVLEFEASQ), 13 (LVT), 14 (FRSGF), 15 (GMR), J (KQNVSLSILKSHE), K (FMEDLDKTW)

B

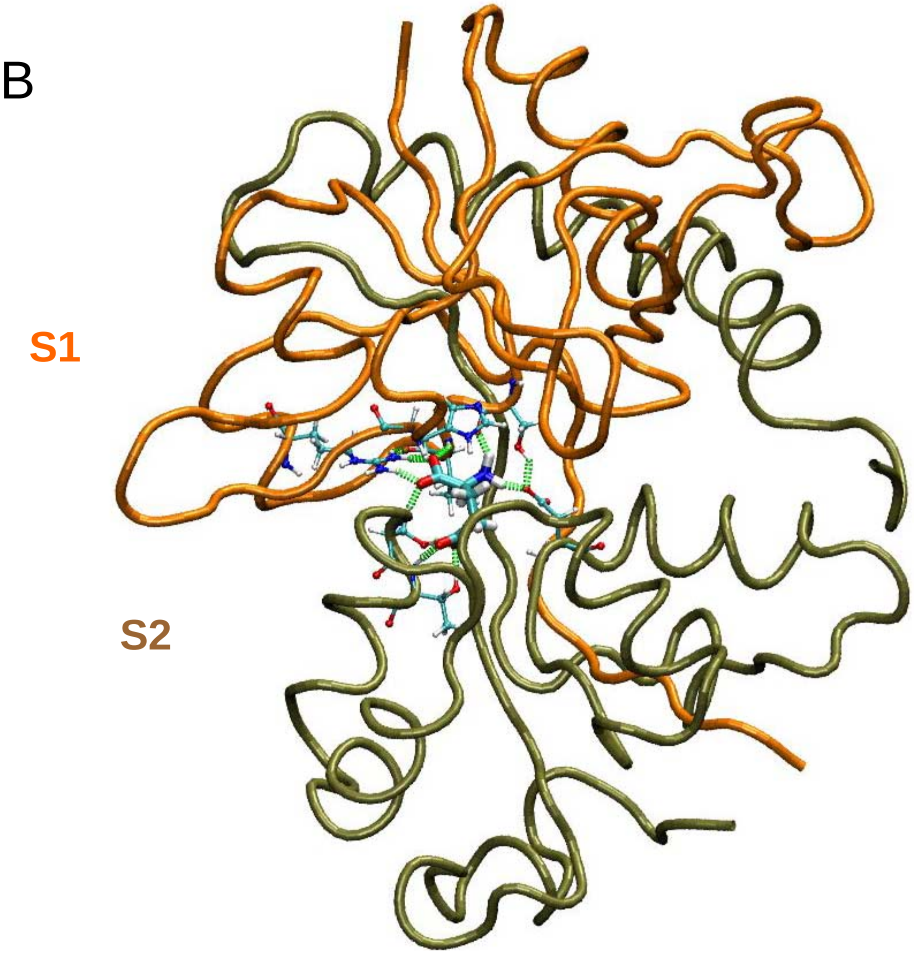

C

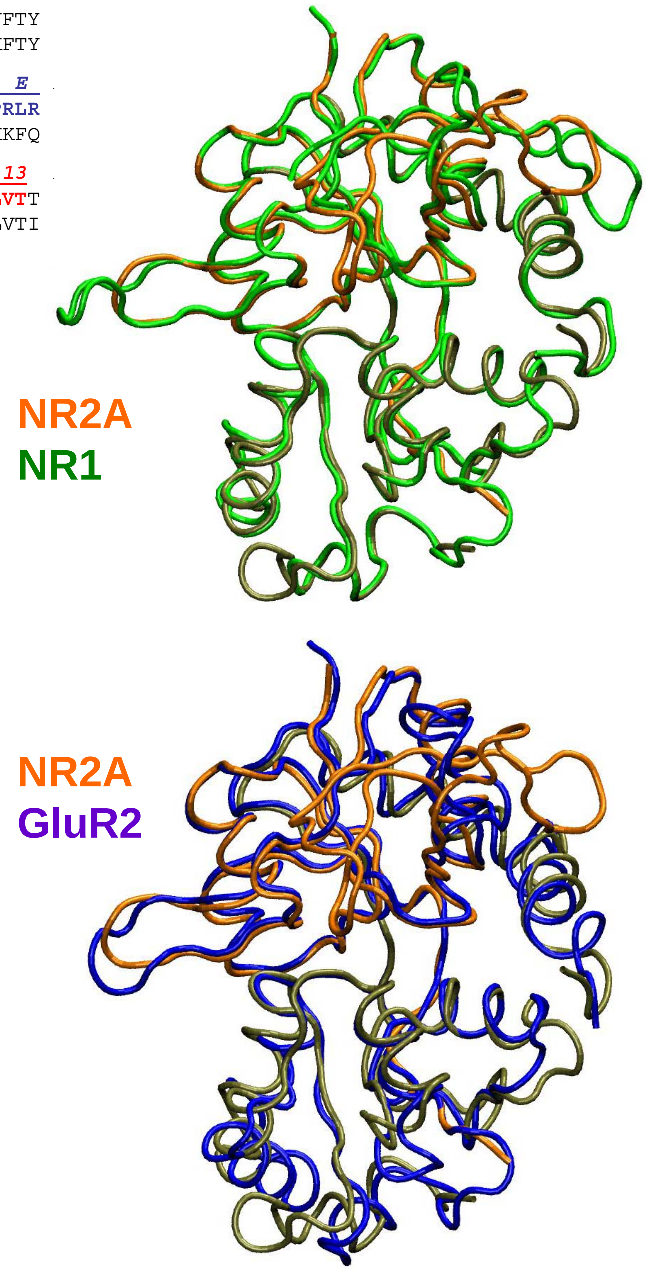

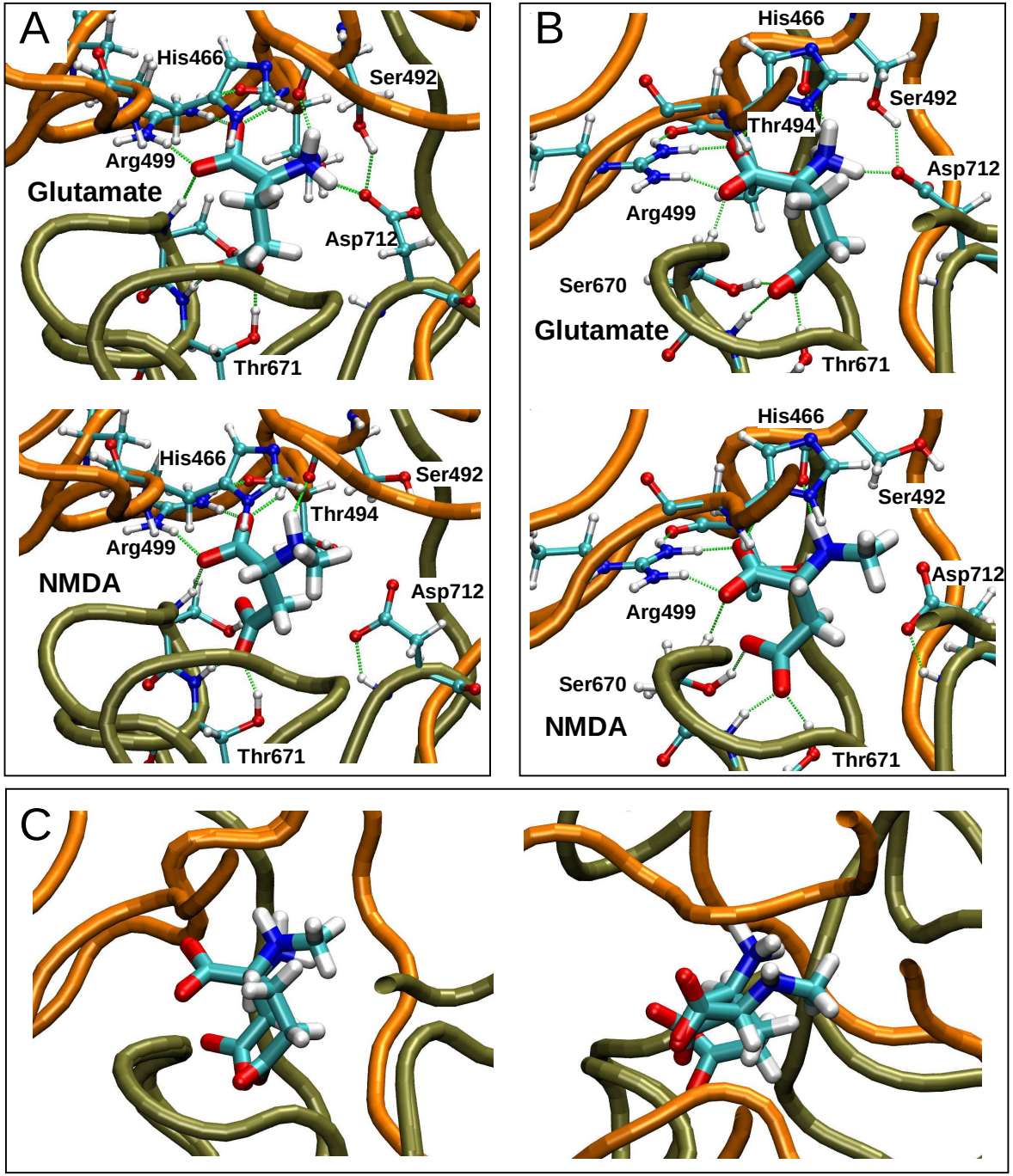
A
His466
Ser492
Arg499
Glutamate
Asp712
Thr671
His466
Ser492
Thr494
Arg499
NMDA
Asp712
Thr671
B
His466
Ser492
Thr494
Asp712
Arg499
Ser670
Glutamate
Thr671
His466
Ser492
Asp712
Arg499
Ser670
NMDA
Thr671
C

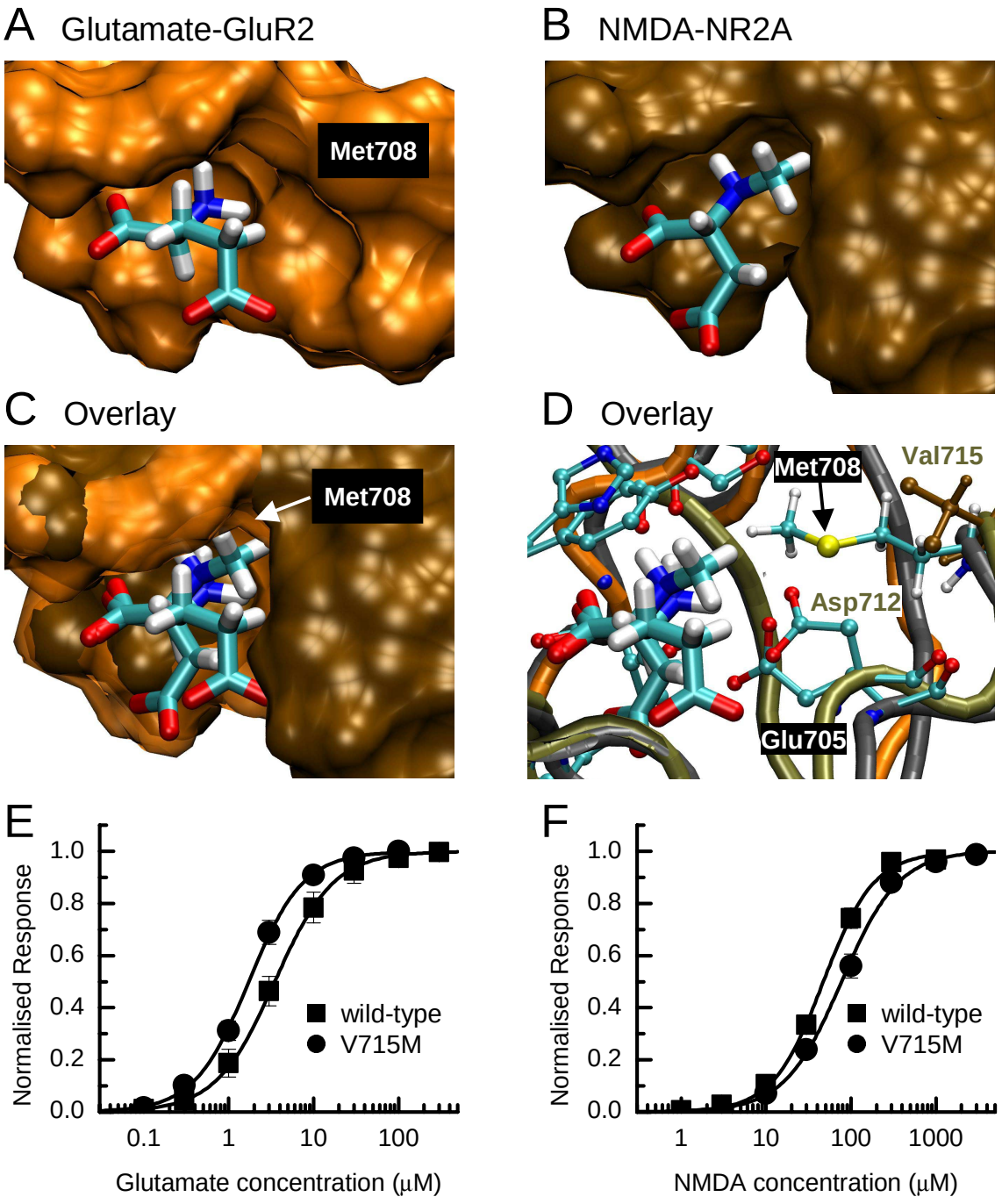
A Glutamate-GluR2
Met708
B NMDA-NR2A
C Overlay
Met708
D Overlay
Met708
Val715
Asp712
Glu705
E
Normalised Response
1.0
0.8
0.6
0.4
0.2
0.0
0.1
1
10
100
wild-type
V715M
Glutamate concentration (μM)
F
Normalised Response
1.0
0.8
0.6
0.4
0.2
0.0
1
10
100
1000
wild-type
V715M
NMDA concentration (μM)

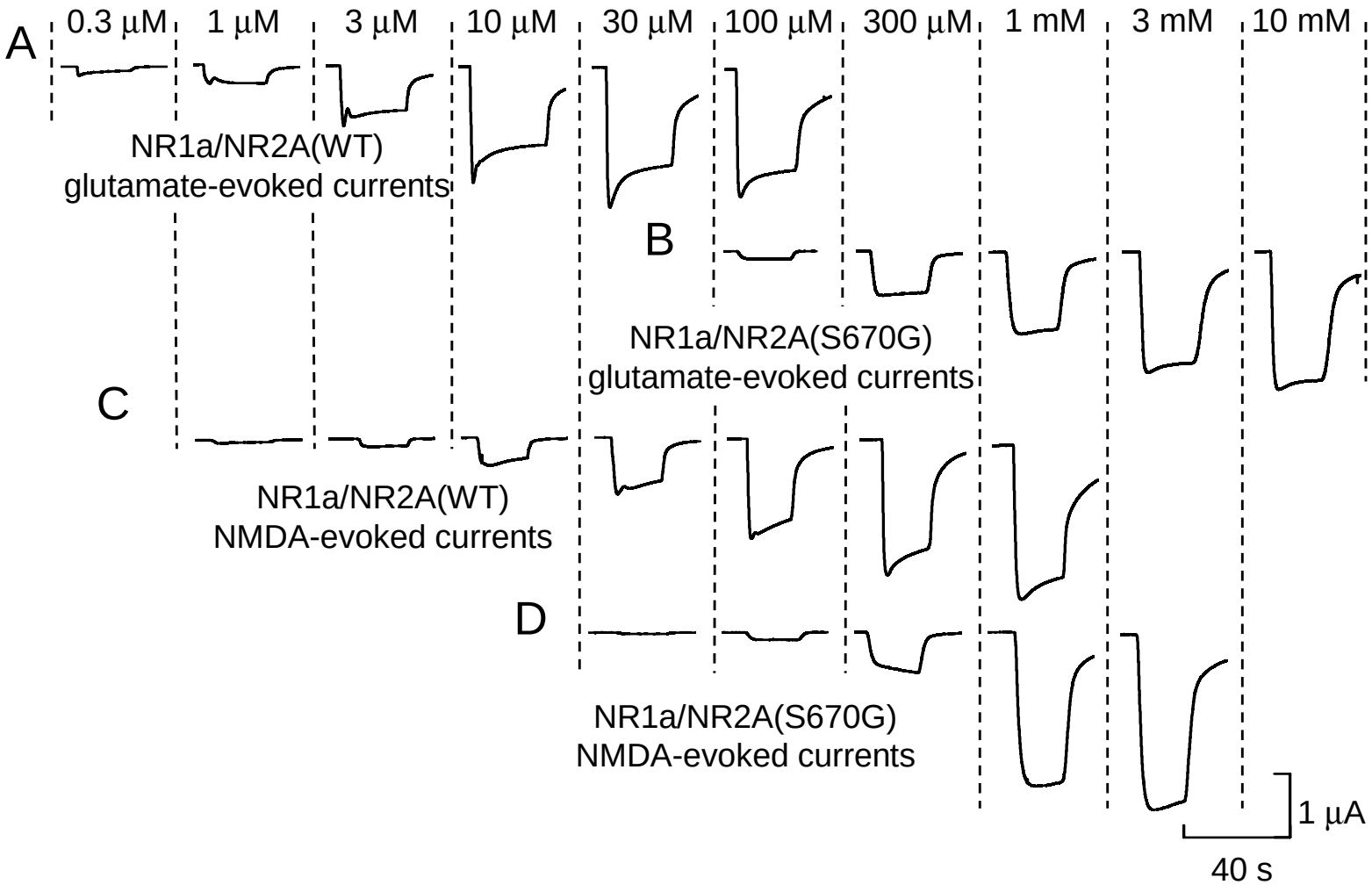
A
0.3 μM
1 μM
3 μM
10 μM
30 μM
100 μM
300 μM
1 mM
3 mM
10 mM
NR1a/NR2A(WT)
glutamate-evoked currents
B
NR1a/NR2A(S670G)
glutamate-evoked currents
C
NR1a/NR2A(WT)
NMDA-evoked currents
D
NR1a/NR2A(S670G)
NMDA-evoked currents
1 μA
40 s

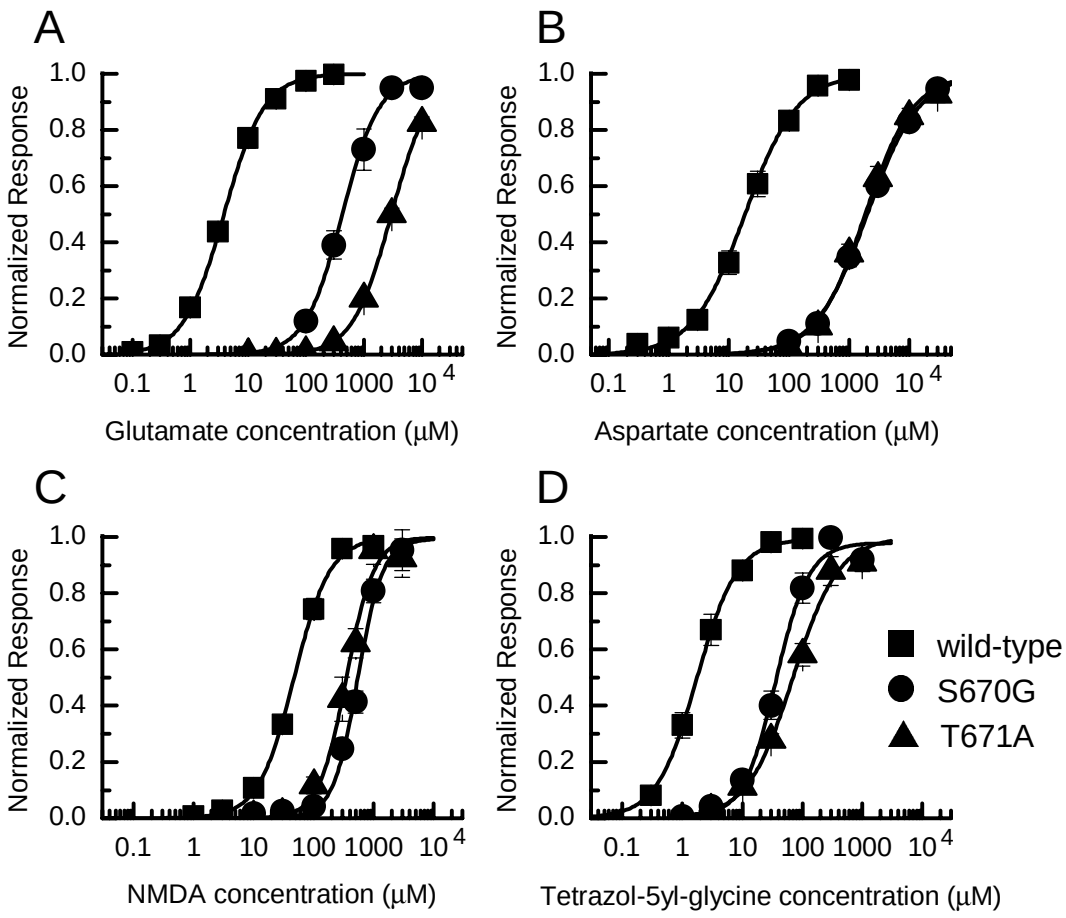
A
B
C
D
Normalized Response
1.0
0.8
0.6
0.4
0.2
0.0
0.1
1
10
100
1000
10 4
Glutamate concentration (μM)
Aspartate concentration (μM)
NMDA concentration (μM)
Tetrazol-5yl-glycine concentration (μM)
wild-type
S670G
T671A

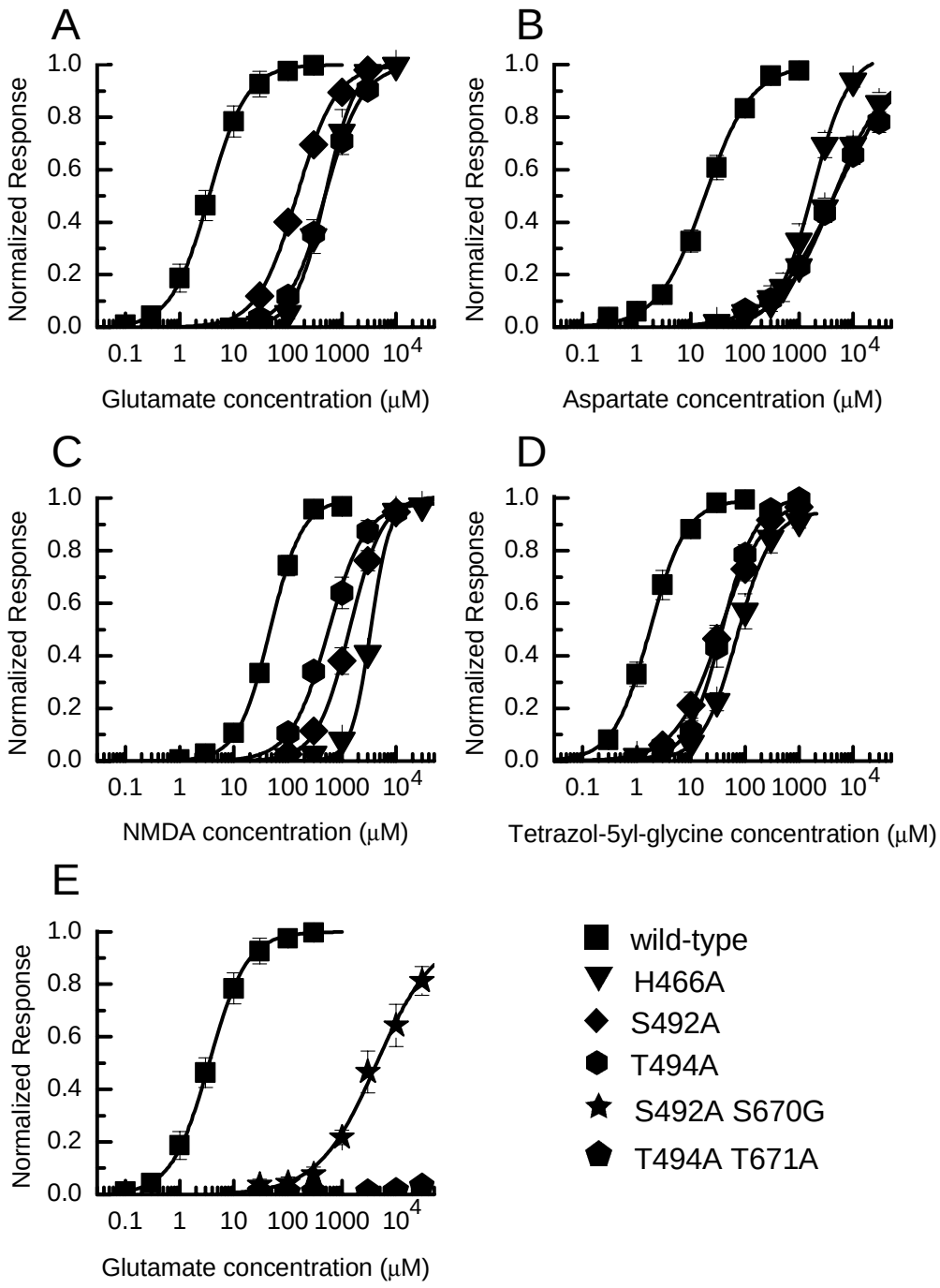
A
B
C
D
E
Normalized Response
1.0
0.8
0.6
0.4
0.2
0.0
0.1
1
10
100
1000
10^4
Glutamate concentration (μM)
Aspartate concentration (μM)
NMDA concentration (μM)
Tetrazol-5yl-glycine concentration (μM)
wild-type
H466A
S492A
T494A
S492A S670G
T494A T671A

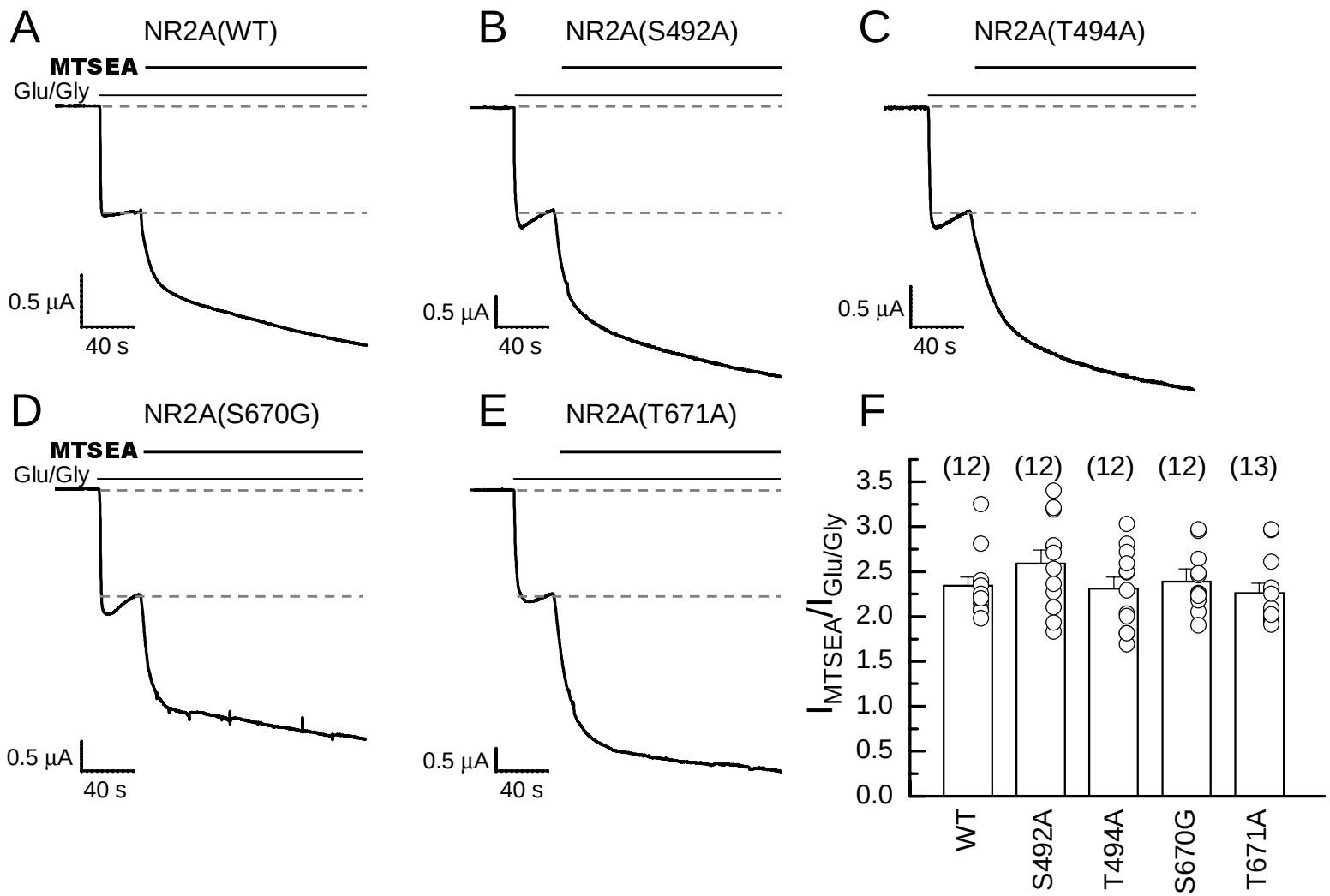
A
NR2A(WT)
MTSEA
Glu/Gly
0.5 μA
40 s
B
NR2A(S492A)
0.5 μA
40 s
C
NR2A(T494A)
0.5 μA
40 s
D
NR2A(S670G)
MTSEA
Glu/Gly
0.5 μA
40 s
E
NR2A(T671A)
0.5 μA
40 s
F
(12)
(12)
(12)
(12)
(13)
$I_{MTSEA}/I_{Glu/Gly}$
3.5
3.0
2.5
2.0
1.5
1.0
0.5
0.0
WT
S492A
T494A
S670G
T671A

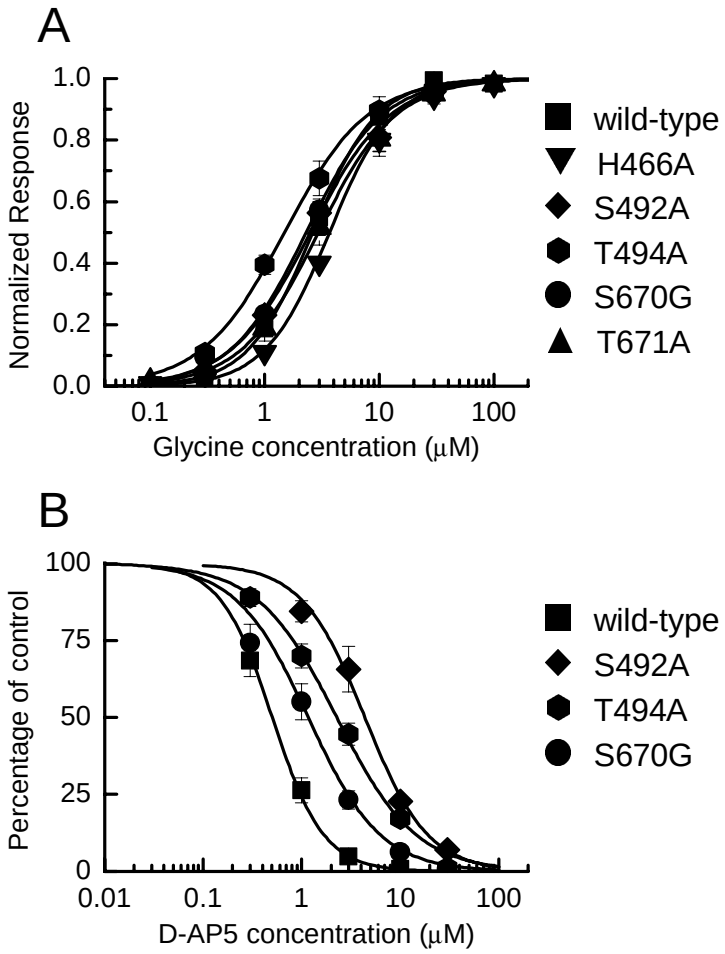
A
1.0
0.8
0.6
0.4
0.2
0.0
Normalized Response
0.1
1
10
100
Glycine concentration (μM)
wild-type
H466A
S492A
T494A
S670G
T671A
B
100
75
50
25
0
Percentage of control
0.01
0.1
1
10
100
D-AP5 concentration (μM)
wild-type
S492A
T494A
S670G

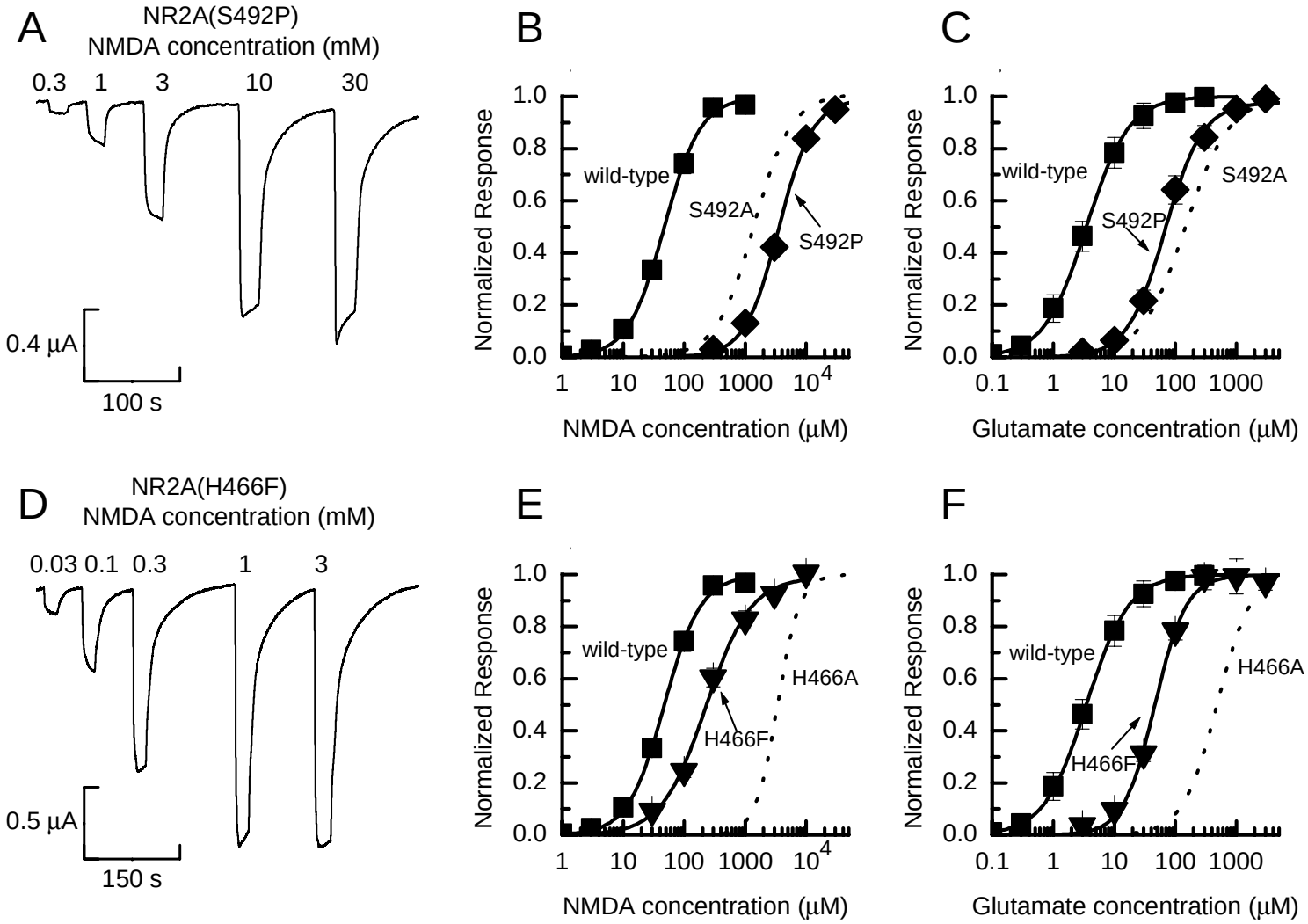
A
NR2A(S492P)
NMDA concentration (mM)
0.3
1
3
10
30
0.4 μA
100 s
B
Normalized Response
wild-type
S492A
S492P
NMDA concentration (μM)
C
Normalized Response
wild-type
S492A
S492P
Glutamate concentration (μM)
D
NR2A(H466F)
NMDA concentration (mM)
0.03
0.1
0.3
1
3
0.5 μA
150 s
E
Normalized Response
wild-type
H466A
H466F
NMDA concentration (μM)
F
Normalized Response
wild-type
H466A
H466F
Glutamate concentration (μM)

A

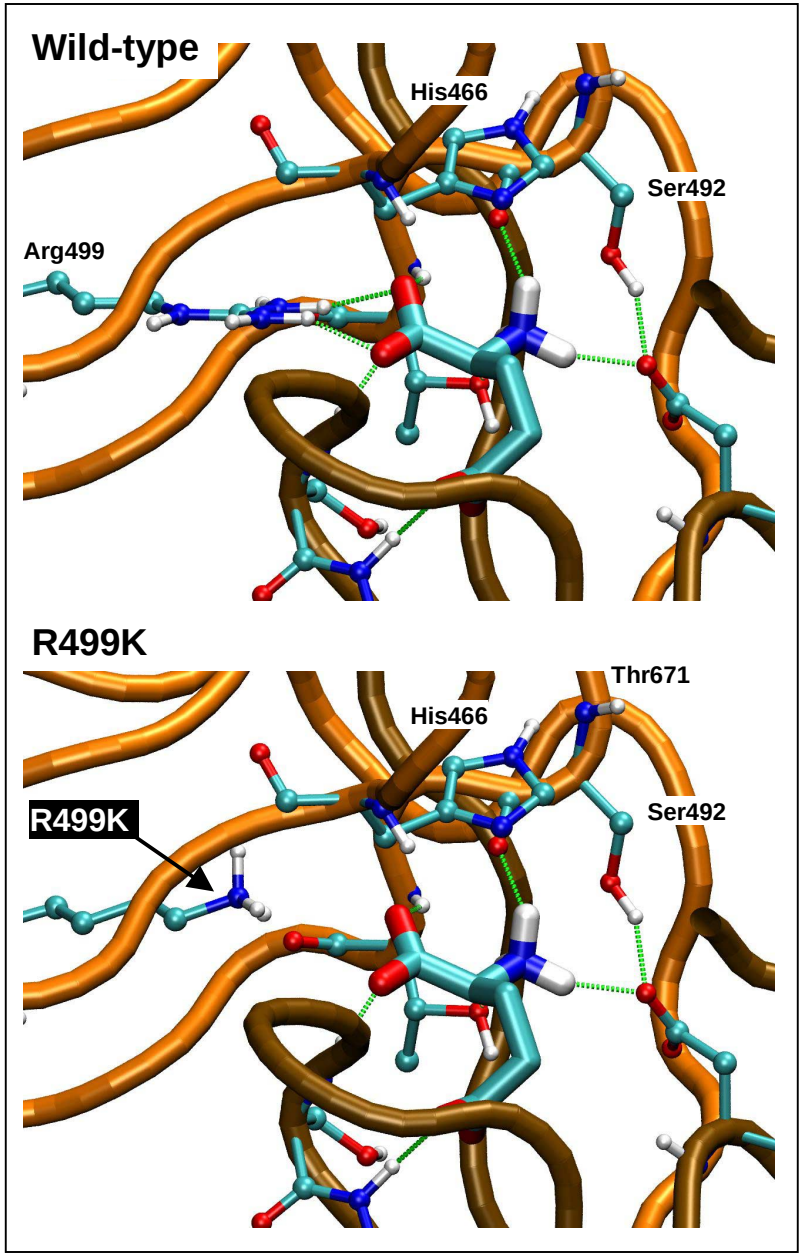
Wild-type
His466
Ser492
Arg499
R499K
Thr671
His466
R499K
Ser492

B

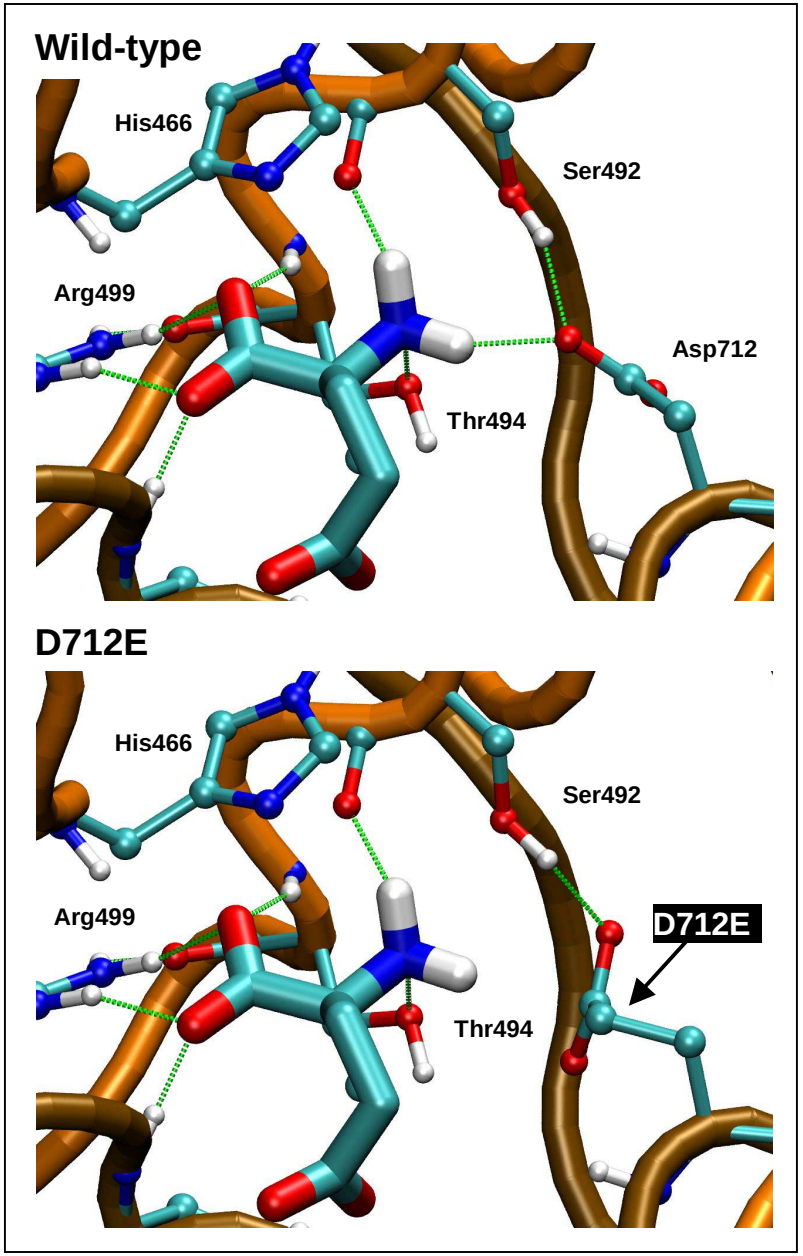
Wild-type
His466
Ser492
Arg499
Asp712
Thr494
D712E
His466
Ser492
Arg499
D712E
Thr494